The Thesis Committee for Glenn Kenneth Makechnie
Certifies that this is the approved version of the following thesis:

Sequence Stratigraphic Analysis of Marginal Marine Sabkha Facies: Entrada Sandstone, Four Corners Region

APPROVED BY

SUPERVISING COMMITTEE:

Supervisor: ______________________________
Gary Kocurek

____
David Mohrig

____
Ronald Steel

Sequence Stratigraphic Analysis of Marginal Marine Sabkha Facies:

Entrada Sandstone, Four Corners Region

by

Glenn Kenneth Makechnie, B.S.

Thesis

Presented to the Faculty of the Graduate School

Of the University of Texas at Austin

In Partial Fulfillment

Of the Requirements

For the Degree of

Masters of Science in Geological Sciences

The University of Texas at Austin

August 2010

Dedication

This thesis is dedicated to my wife, Kim, for encouraging me, to my mother, for teaching me how to wonder, and to my father, for always putting his family first.

Acknowledgements

I would like to acknowledge the help of my supervisor, Gary Kocurek, without whom this study would have been impossible. Thank you to the Minerals department of the Navajo Nation for granting permits to access Navajo Nation land for this study. Thank you to ExxonMobil for funding field work, and to my father-in-law, David Hansen, who allowed me to use his truck. Also, thanks to Thomas Charles Brothers, Erin Eastwood, and Ryan Ewing for assistance in the field.

August 2010

Abstract

Sequence Stratigraphic Analysis of Marginal Marine Sabkha Facies: Entrada Sandstone, Four Corners Region

Glenn Kenneth Makechnie, MSGeoSci
The University of Texas at Austin, 2010

Supervisor: Gary Kocurek

Abstract: The Middle Jurassic Entrada Sandstone of the Four Corners region, USA, is composed predominantly of very fine-grained, red, silty sandstone with poorly defined sedimentary structures. The origin of this facies is enigmatic, even though it is common both on the Colorado Plateau and globally, and is spatially situated between deposits recording unambiguous marine and aeolian environments. Eleven sections were measured along an 85 km transect from the Blanding Basin in southeastern Utah to the San Juan Basin in northwestern New Mexico. Outcrop and laboratory analyses distinguish eight facies: (1) silty shale, (2) shallow subaqueous reworked, fine- to medium-grained sandstone, (3) brecciated, very fine-grained sandstone, (4) crinkly laminated, very fine-grained sandstone with preserved wind ripples and abundant silty laminae, (5) weakly laminated, fine-grained sandstone with occasional silty laminae, (6) planar-laminated, fine-grained, wind-rippled sandstone, (7) cross-stratified, fine- to medium-grained aeolian cross-stratified sandstone, and (8) micritic limestone. Lateral and vertical relationships of these facies show a proximal to distal transition from cross-bedded wind-lain facies to loess-dominated sabkha facies with increasing abundance of water-lain facies basinward. The well known Todilto Limestone (facies 8) is situated stratigraphically below loess-dominated sabkha facies (facies 4 and 5) within the Entrada

Sandstone, reinforcing previous interpretations that the unit represents a catastrophic flooding event and not a local groundwater flux.

Table of Contents

List of Figures

INTRODUCTION

A common facies that occurs between clear aeolian and marine sedimentary accumulations within Jurassic strata on the Colorado Plateau of the United States consists of a red, fine-grained sandstone with poorly defined sedimentary structures. This transitional facies has been described as “silty to massive” (O’Sullivan, 1978) and interpreted as representing “sabkha” deposition (Imlay, 1980; Kocurek and Dott, 1983; O’Sullivan and Pierce, 1983; Blakey et al., 1988; Peterson, 1988), but its exact origins remain unknown. This facies is volumetrically significant in the Middle Jurassic Entrada Sandstone (Kocurek and Dott, 1983; Blakey et al, 1988), especially in the area of the Four Corners of the United States, where it constitutes nearly the entirety of the formation. To first-order, the Jurassic red, fine-grained sandstones are similar to strata in the Pennsylvanian-Permian Maroon Formation of the Eagle Basin in northwestern Colorado, which have been interpreted as loess deposits (Johnson, 1987, 1989; Soreghan et al., 2008) and to the beds of the early Pennsylvanian-Permian Cutler Formation of the Paradox Basin in, Utah (Johnson, 1989). Loess is characterized by sediments finer than 62 µm, the cutoff for aeolian suspended sediment, and can be carried tens of kilometers from dune fields by normal winds (Tsoar and Pye, 1987; Pye, 1995). The amount of loess present within facies of enigmatic origin is used in its interpretation.

This study uses a combination of outcrop descriptions, regional stratigraphic relationships, and grain-size analysis to interpret the red, fine-grained sandstones of the Entrada Sandstones in the Four Corners area. Sedimentary structures and grain-size analysis show that distinct subfacies can be recognized and traced laterally as coherent units. Interpretation of the depositional environments associated with these subfacies can be made by their placement within a regional stratigraphic framework that contains facies of known origins. In addition, the Todilto Limestone pinches out within the study area. The Todilto Limestone is a well known but enigmatic unit that has been interpreted to represent a catastrophic flooding of the Entrada Dune Field (Benan & Kocurek, 2000). This study demonstrates the environment in which this flooding event occurred and the timing of this event with respect to overall Entrada stratigraphy.

TECTONIC AND STRATIGRAPHIC SETTING

Deposition of the Entrada Sandstone in the Four Corners region was influenced by spatial variations in subsidence associated with the San Juan and Blanding Basins, the Uncompaghre Uplift, the Defiance-Zuni Arch, and the Monument Arch (Fig. 1A). These features developed during the Pennsylvanian-Permian with deformation associated with the formation of the Ancestral Rocky Mountains (Kelley, 1950; Mallory, 1958; Mallory, 1972; Kluth and Coney, 1981; Baars et al., 1988; Ye et al., 1996). The Blanding Basin is a sub-basin of the Paradox Basin, which is a structural depression associated with the formation of the adjacent Uncompaghre Uplift, an element of the Ancestral Rocky Mountains (Mallory, 1958; Wengerd and Matheny, 1958; Stevenson and Baars, 1986; Barbeau, 2003). The Blanding Basin is separated from the Henry Mountains Basin, another Paradox sub-basin, by the Monument Arch (Ohlen and Mcintyre, 1965; Wengerd and Matheny, 1958), and from the San Juan Basin by the Defiance-Zuni Arch and a low platform in the Four Corners Region (Kelley, 1950; Huffmann and Condon, 1993). Regional facies relationships and stratigraphic thicknesses argue that these structural features were active during the Jurassic, and have been tectonically significant since at least Pennsylvanian-Permian time (Blakey, 1988). Within the study area, thickest Jurassic accumulations occur within the Blanding and San Juan Basins, with marked thinning over the Defiance-Zuni Arch along the Arizona-New Mexico boarder accompanied by facies change within Jurassic strata (Cooley et al. 1969; Figs. 1B, 2).

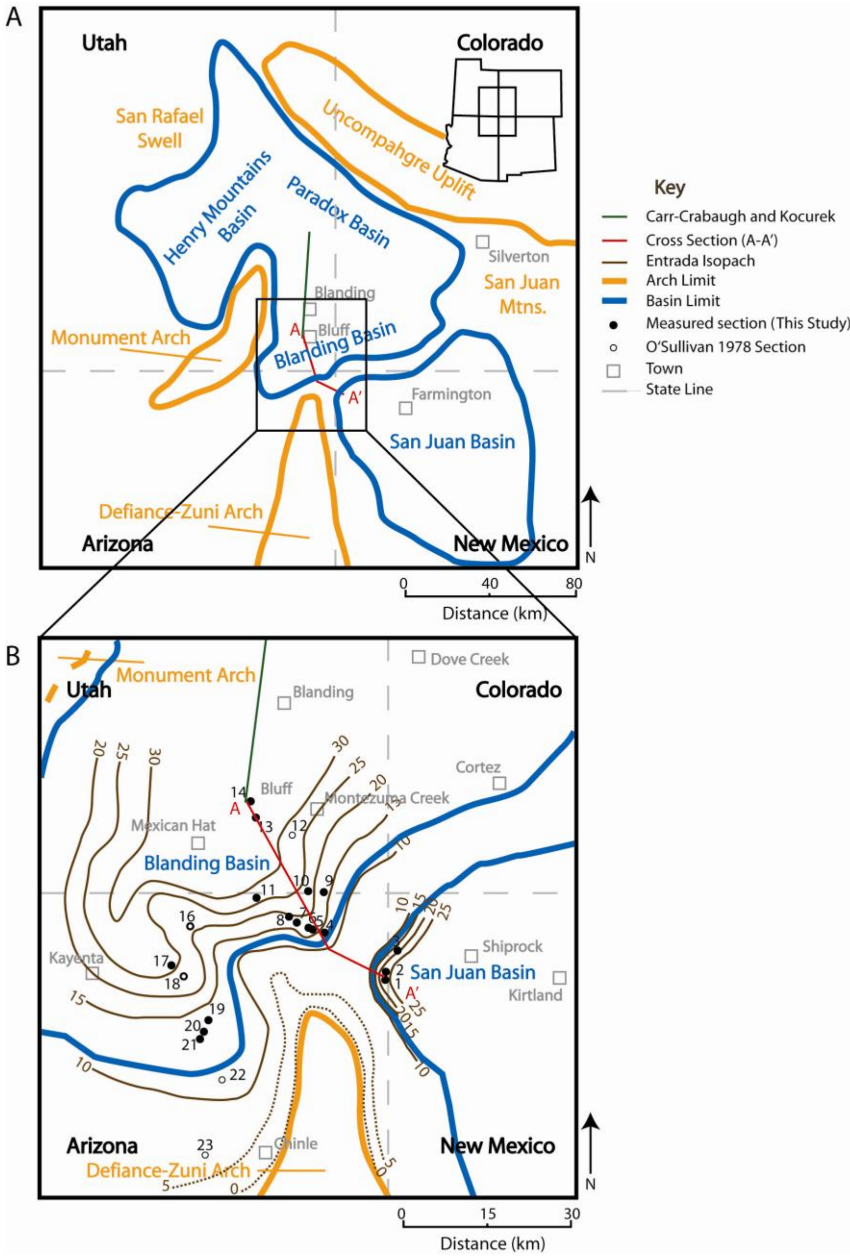

Fig. 1- (A) Paleo-structural elements of the Four Corners Region (USA), shows spatial distribution of elements affecting Middle Jurassic sedimentation and location of transects of this study and Carr-Crabaugh and Kocurek (1998). Entrada thicknesses measured in this study are supplemented by additional sections from O'Sullivan (1978). (B) Measured section locations and Entrada Sandstone isopach in the Four Corners Region showing Entrada thickness in the Blanding and San Juan Basins with thinning across the Defiance Ridge from A-A'. Isopach measurements in meters. Modified from Woodward (1984), Blakey (1998), and Woodward et al. (1997).

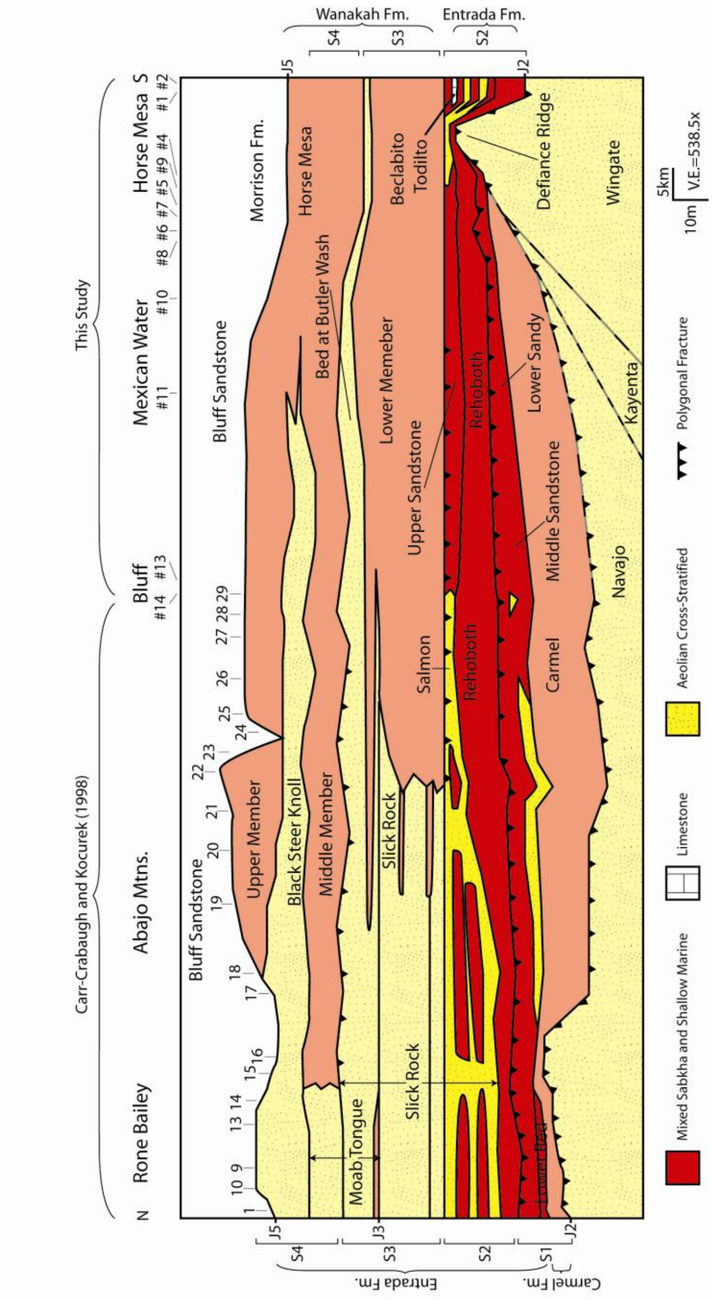

Fig. 2- General stratigraphy and facies relationships for the San Rafael Group showing aeolian-dominated environments in eastern Utah grading southward into marine-sabkha-dominated environments southward into the Four Corners Region. Units addressed in this study are highlighted in bright colors. Modified from Blakey (1988), Spencer and Lucas (1997), and Carr-Crabaugh and Kocurek (1998).

The Entrada Sandstone is a Jurassic unit within the Bathonian-Late Callovian San Rafael Group, a sedimentary unit composed within the study area of southward prograding aeolian sands inter-tonguing with shallow marine deposits (Harshbarger et al., 1957; O'Sullivan, 1980; Carr-Crabaugh and Kocurek, 1998). Within the study area, the San Rafael Group is bounded by the J2 and J5 unconformities (Pipringos and O'Sullivan, 1998). Carr-Crabaugh and Kocurek (1998) described four sequences within the San Rafael group of eastern Utah that consist of basal sabkha-dominated depositional systems overlain by migrating cross-stratified dune and interdune facies and capped by polygonally fractured or featureless surfaces (Fig. 2). This study traces two sequences of Carr-Crabaugh and Kocurek (1998) from the Blanding Basin near Bluff, Utah, across the Defiance-Zuni Arch into the San Juan Basin in northwestern New Mexico (Fig 2).

The "basal sabkha-dominated depositonal system" of sequence I of Carr-Crabaugh and Kocurek (1998) is the Carmel Formation, a succession of vertically stacked shallow marine and thin aeolian dune deposits that record the Carmel transgression and correlate laterally within the Dewy Bridge Member of the Entrada Sandstone (Peterson, 1986). These deposits are overlain by the basal member of the Entrada Sandstone, the Middle Sandstone/Lower Sandy Member, which is capped by a polygonal fracture surface. Sequence II is composed of the next two members of the Entrada Sandstone: the Rehoboth Member and the Upper Sandstone/Salmon Member, which is capped by another polygonally fractured surface. The Entrada Sandstone is overlain by the youngest unit of the San Rafael Group, the Wanakah Formation (or Summerville Formation), which is capped by the J5 unconformity (Harshbarger et al., 1957; O'Sullivan, 1980; Fig. 2). The Wanakah Formation inter-tongues northward with the remainder of the Entrada Sandstone, the Slick Rock Member, Moab Tongue, and Black Steer Knoll Member (Fig. 2). The Todilto Limestone is a member of the San Rafael Group within the San Juan Basin of New Mexico, Arizona and Colorado, and its specific stratigraphic location will be discussed later in this paper.

While controversy surrounds correlation and naming of members within the Entrada Sandstone of the Four Corners area, stratigraphic nomenclature for the three members of the Entrada Sandstone that exist within this study area is adopted from most recent USGS publications (O'Sullivan, 1978; O'Sullivan, 1980; Robertson and O'Sullivan, 2000, 2001), and are, in order from oldest to youngest; Lower Sandstone or Middle Sandstone Member, Rehoboth Member, and Upper Sandstone or Salmon Member (Fig. 3). A change in nomenclature for the lower and upper members of the Entrada occurs at the border of the Navajo Nation in southern Utah, where the Upper Sandstone Member becomes the Salmon Member, and the Lower Sandy Member becomes the Middle Sandstone Member crossing the San Juan River from south to north (Figs. 2, 4). Alternative nomenclature, proposed by Lucas et al. (1998; Fig. 3), is rejected here because it fails to conform to stratigraphic units that are traceable in the field.

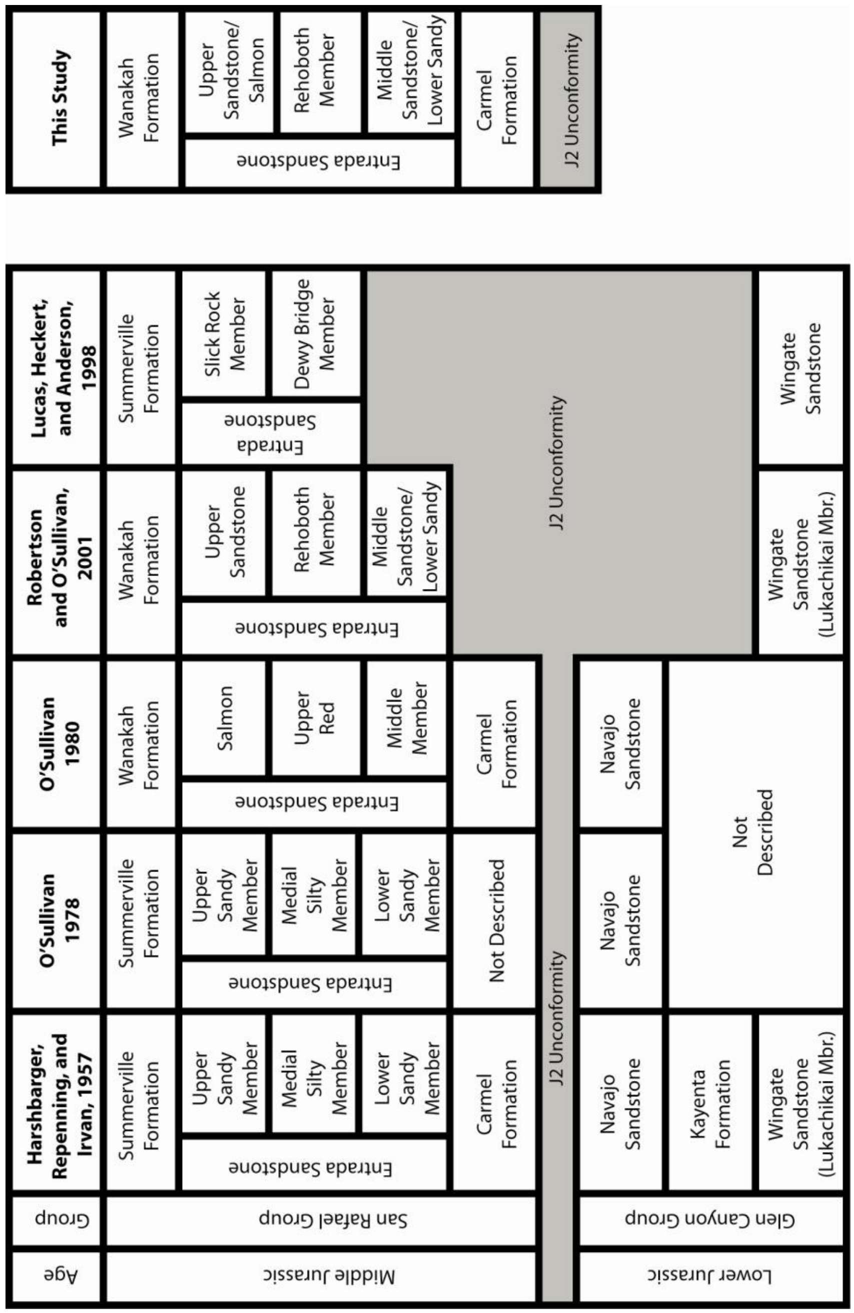

Fig. 3- Summary of evolution of stratigraphic nomenclature for several Middle Jurassic Units in this study. This study adopts most recent USGS nomenclature (Robertson and O'Sullivan, 2001) because it conforms to stratigraphic relationships that are traceable in the field, and that are confirmed by sedimentalogic analysis.

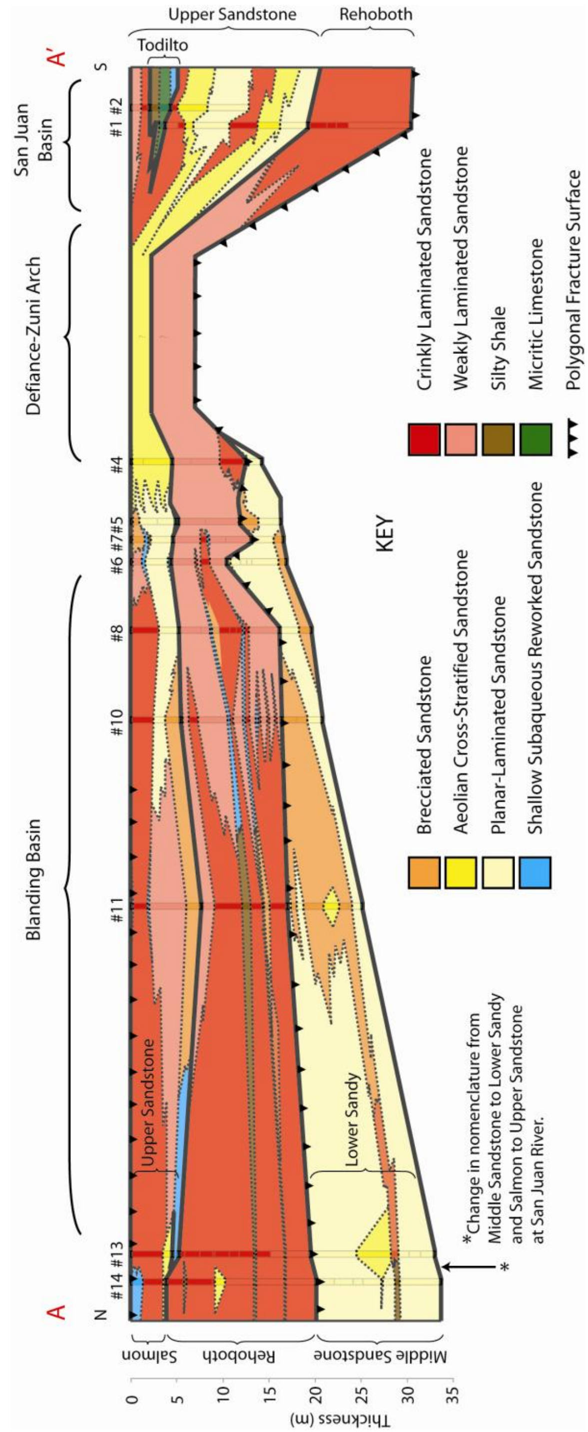

Fig. 4- A transect from A-A' (Fig. 1B) using 11 measured sections with the Blanding and San Juan Basins shows vertical and lateral relationships of 8 facies identified within the Entrada Sandstone as well as thinning and facies changes associated with the paleo-topography of the Defiance-Zuni Arch.

FACIES DESCRIPTIONS

Facies were distinguished in outcrop and in hand sample by subtle differences in sedimentary structures and grain size (Figs. 5, 6). These descriptive facies are separated into “facies of known origin”, representing units with recognizable environmental affinity, and “facies of unknown origin”.

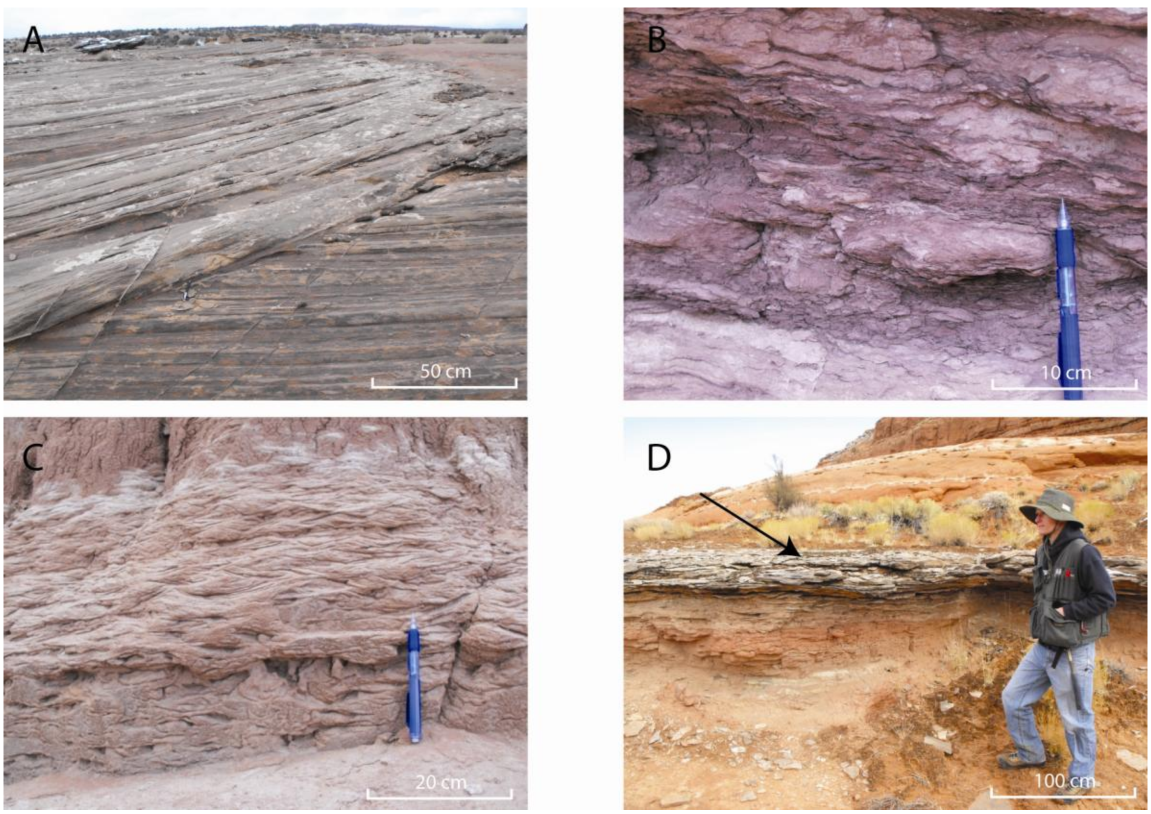

Fig. 5- Facies of known origin: (A) Aeolian Cross-Stratified Sandstone, (B) Silty Shale, (C) Shallow Subaqueous Reworked Sandstone, and (D) Micritic Limestone, with arrow pointing to limestone. Facies of unknown origin: (E) Planar-Laminated Sandstone, with arrows pointing to (a) coarse-grained laminations, interpreted as lag surfaces, and (b) inversely-graded laminations, interpreted as ripple laminae, (F) Brecciated Sandstone, with mm-scale euhedral salt dissolution vugs, (G) Weakly Laminated Sandstone, with arrows showing discontinuous silty red laminae, and (H) Crinkly Laminated Sandstone, with arrows showing laterally continuous red silty laminations.

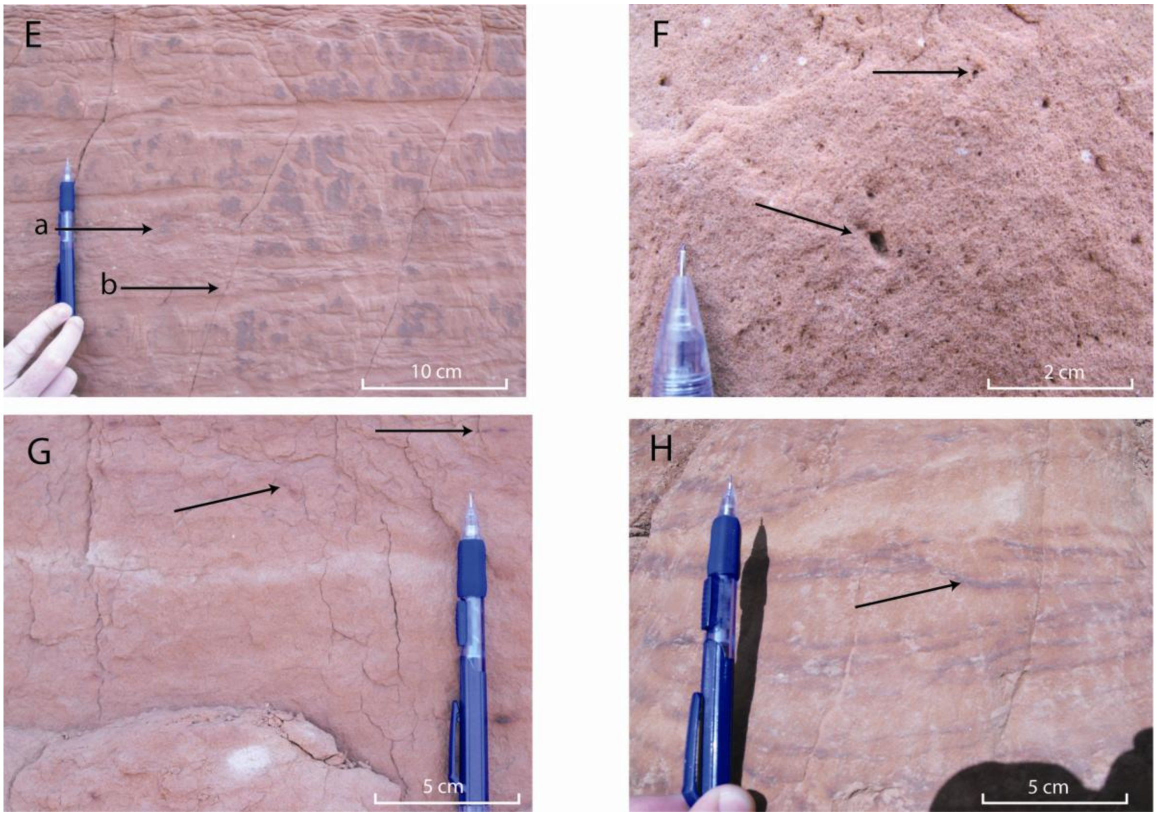

Fig. 5 cont.

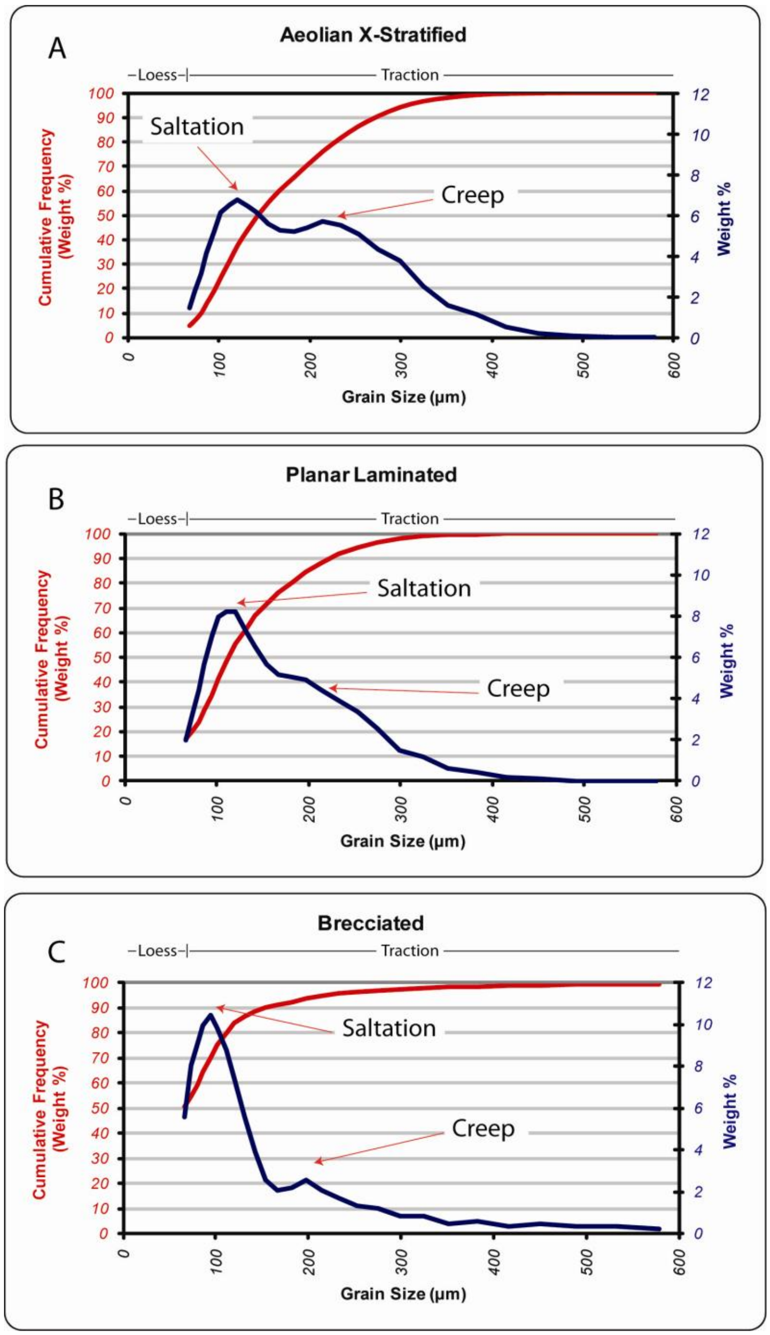

Fig. 6- Grain size analysis of (A) Aeolian Cross-Stratified Sandstone, (B) Planar Laminated Sandstone, (C) Brecciated Sandstone, (D) Weakly Laminated Sandstone, and (E) Crinkly Laminated Sandstone. Grain size distributions are reported as weight percent of only the sand fraction coarser than 62 µm for each sample, while the cumulative frequency curve includes weight percent of grains finer than 62 µm. Statistics are reported based on analysis of grains coarser than 62 µm only. For analysis, grains finer than 62 µm are considered suspended load, or "loess", grains coarser than 62 µm are considered traction load (Pye and Tsoar, 1987). See text for analysis of grain size trends

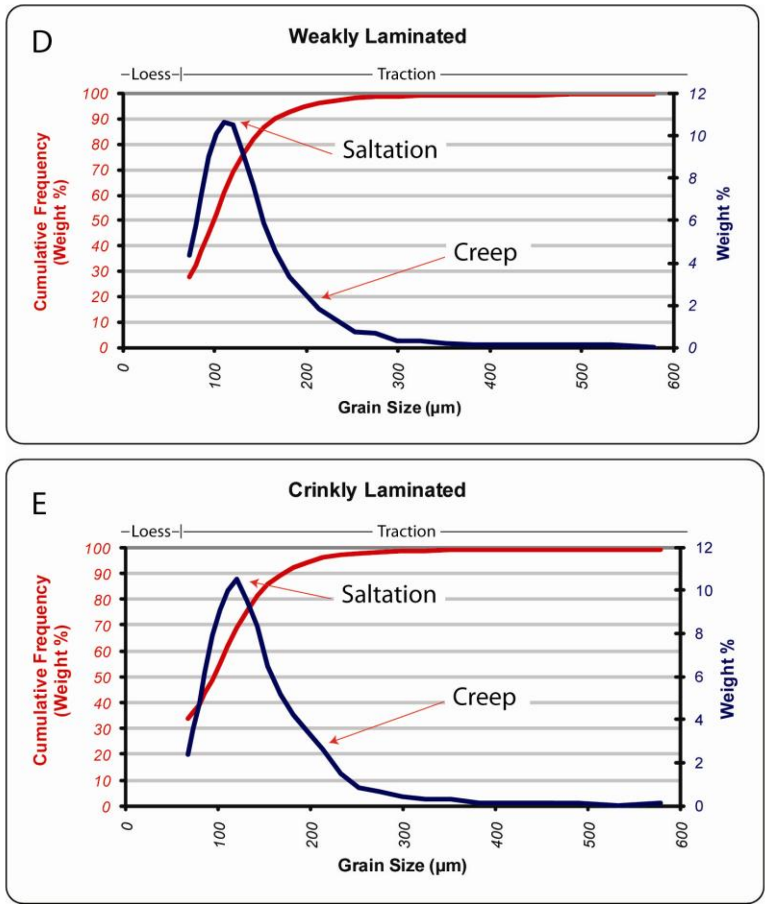
D
Weakly Laminated
Loess
Traction
Saltation
Creep
Cumulative Frequency (Weight %)
Weight %
Grain Size (μm)
E
Crinkly Laminated
Loess
Traction
Saltation
Creep
Cumulative Frequency (Weight %)
Weight %
Grain Size (μm)

Fig. 6 cont.

Facies of Known Origin

FACIES 1: CROSS-STRATIFIED SANDSTONE

An aeolian cross-stratified sandstone forms resistant, tan-colored outcrops up to 5 m thick with sub-meter scale (10-30 cm), wind-rippled, resistive beds of cross-strata (Fig. 5A). Where the facies overlies silty units, the lower contact is undulating, interpreted as resulting from soft-sediment deformation, and the lower ~ 20 cm of the sand is typically marked by a concentration of coarse-grains, interpreted as a lag deposit similar to those commonly observed in modern environments (Kocurek and Nielson, 1986; Fryberger et al., 1992). Cross-strata show a general dip direction of 200°, corresponding with a regional southward dune migration for the Entrada (Peterson, 1988). Grains are well-rounded and frosted, and the sediment is fine-grained, moderately sorted, and coarse-skewed, with a distinct bimodal distribution thought to reflect sand transport by both saltation and creep processes (Tsoar and Pye, 1987; Fig. 6A). By weight, the potential suspended load, taken as silicate particles with nominal diameters < 62 µm, is less than 10%, which is typical of dune sand (Glennie, 1970).

The Aeolian Cross-Stratified Sandstone Facies occurs primarily within the Upper Sandstone Member of the Entrada Sandstone, specifically over the Defiance-Zuni Arch (Fig. 4). This facies is significant for the development of a framework for interpreting facies of unknown origin, because it is the only facies within the study area that represents aeolian dune-field accumulations. From the Defiance-Zuni Arch northwestward into the Blanding Basin, the facies thickens somewhat, but terminates by inter-tonguing with the Planar-Laminated Facies (Fig. 4). The facies can be traced southwestward from the Defiance-Zuni Arch into the San Juan Basin, where it is underlain by the Planar-Laminated Facies and overlain by the Crinkly Laminated Sabkha Facies. Isolated pods of the Aeolian Cross-Stratified Facies are also found within the Blanding Basin, primarily within the Lower Sandy Member, encased within the Planar-Laminated or Brecciated Facies. These small pods of strata are interpreted as isolated dunes migrating across these other environments.

FACIES 2: SILTY SHALE

The Silty Shale Facies is composed of dark-red mudstone laminations of varying thickness that are intermixed with pink to red, very fine-grained to silty sandstone laminations. Sandstone laminations commonly contain critically climbing or bi-directional subaqueous ripple cross-strata. Laminations of sandstone and mudstone are 0 to 10 cm thick, laterally discontinuous and undulating. Biotite grains of very fine sand size are common within the dark red, muddy portion of this facies.

The Silty Shale Facies occurs as sub-meter thick, laterally continuous strata, and is found predominantly within the most distal portions of the Blanding Basin within the Rehoboth Member where it transitions to the Shallow Subaqueous Reworked Sandstone Facies. It is also observed within the Lower Sandy/Middle Sandstone Member where it laterally interfingers with Crinkly Laminated Sandstone Facies (Fig. 4). Within the San Juan Basin, the Silty Shale Facies overlies the Micritic Limestone Facies of the Todilto flooding event. This study demonstrates that this unit of Silty Shale is included within the Upper Sandstone Member of the Entrada Sandstone, and does not represent the beginning of the Wanakah Formation. In both basins the Silty Shale Facies is interpreted as sediment accumulation in a shallow marine environment based on the mixture of mud and sand deposits and on its distal position relative to other subaqueous environments represented by the Shallow Subaqueous Reworked Sandstone Facies.

FACIES 3: SHALLOW SUBAQUEOUS REWORKED SANDSTONE

The Shallow Subaqueous Reworked Sandstone Facies is a composite facies that everywhere shows evidence for water reworking. The unit is typically less than 1 m thick, and consists of sub- to well-rounded sand, which varies in size from very fine- to coarse-grained sand. Bi-directional and mud-draped ripple cross-strata are common within this facies, as well as 10 cm thick subaqueous dune cross-strata that commonly contain 2 cm diameter concretions (Fig. 5C).

The Shallow Subaqueous Reworked Sandstone Facies occurs within the Rehoboth and Upper Sandstone Members and correlates basinward with the Silty Shale Facies or Crinkly Laminated Facies and landward with the Brecciated Facies or Weakly Laminated Facies t are characteristic of the Defiance-Zuni Arch (Fig. 4.). The Shallow Subaqueous Reworked Sandstone Facies, along with the Silty Shale Facies, is interpreted to represent shallow marine transgression of sabkha and aeolian environments. The varying grain size of this facies is thought to reflect shallow marine wave and current reworking of sediments previously deposited within a variety of environments.

Facies 4: Micritic Limestone (Todilto Limestone)

The Micritic Limestone Facies is composed of a dark-gray, massive- to wavy-bedded limestone (Fig. 5D). Within the study area this limestone is composed of a basal bi-directional ripple-laminated, calcareous silty sandstone that grades upward into more massive, wavy-bedded, ~ 1 m thick limestone. The Micritic Limestone Facies is found exclusively within the Upper Sandstone Member within the San Juan Basin, where it is the most proximal expression of the Todilto Formation. From the pinchout of the Todilto Limestone at the margins of the San Juan Basin in Beclabito Dome area of northwestern New Mexico, the unit thickens into approximately 15 m of gypsum and limestone in the central portions of the San Juan Basin (Benan and Kocurek, 2000). As discussed more fully below, the Micritic Limestone Facies and its associated Silty Shale Facies are enclosed within the Crinkly Laminated Facies.

Facies of Unknown Origin

Facies 5: Planar-Laminated Sandstone

The Planar-Laminated Sandstone Facies forms tan to pink-colored, up to 8 m thick units, characterized by parallel to sub-parallel, inversely graded laminations. These are interpreted as wind-ripple laminae, with occasional coarse-grained surfaces that are interpreted as lag surfaces (Fig. 5E). The wind-ripple features occur as 2-10 mm thick, very fine-grained laminations, and less common, 3-4 mm thick, coarse-grained laminations. Grains are well-rounded and frosted, identical to those in the Cross-Stratified Sandstone Facies, but the Planar-Laminated Facies shows a distinct fining, represented primarily by a decrease in the interpreted creep load, and a higher proportion (20%) of grains finer than 62 μm (Fig. 6B).

As described above, the Planar-Laminated Facies occurs basinward of the Cross-Stratified Facies, either inter-tonguing with or underlying the latter facies. Yet basinward in the Blanding Basin, the Planar-Laminated Sandstone Facies laterally transitions into the Brecciated or Weakly Laminated Sandstone Facies in the Upper Sandstone Member (Fig. 4). The Planar-Laminated Sandstone Facies is predominant in the Lower Sandy/Middle Sandstone Member within the Blanding Basin where it inter-tongues with the Brecciated Sandstone Facies.

Given the predominance of wind-ripple strata and lag deposits, the increase in proportion of suspended sediment, and its stratigraphic position, the Planar-Laminated Sandstone Facies is interpreted as sand sheet deposits that accumulated in a transitional environment between more proximal dune fields and more distal, subaqueous-dominated environments.

FACIES 6: BRECCIATED SANDSTONE

The Brecciated Sandstone Facies occurs as tan to red, 1-2 m thick sandstone intervals characterized by abundant millimeter-scale, euhedral rectangular vugs. Original sedimentary structures of this facies are difficult to interpret because of soft-sediment deformation, which gives the sandstone a brecciated or contorted appearance (Fig. 5F). Grains are well- to sub-rounded, and very fine- to medium sand with a mode of 86-94 μm and a mean grain size of 106 μm. This facies is distinct from other facies in its high suspended load fraction (~50 % of deposits by weight is <62 μm in diameter) (Fig. 6C).

The Brecciated Sandstone Facies is common within the Middle Sandstone/Lower Sandy and Upper Sandstone Members of the Blanding Basin. It occurs in much smaller quantities within the Rehoboth Member, and is absent in the Upper Sandstone Member of the San Juan Basin. As indicated above, this facies laterally inter-fingers with Planar-Laminated Sandstone Facies of sand sheet origin in the vicinity of the Defiance-Zuni Arch, and inter-fingers basinward with the Shallow Subaqueous Reworked Sandstone or Crinkly Laminated Facies (Fig. 4).

The regional placement of the Brecciated Sandstone Facies within the greater study area is key to its environmental interpretation. Within the Lower Sandy/Middle Sandstone Member the Brecciated Sandstone Facies occurs as the distal expression of a southward prograding tongue of aeolian sand associated with Sequence I (Carr-Crabaugh and Kocurek, 1998) and pinches out against the Defiance-Zuni Arch (Figs 2, 4). These aeolian strata seem best associated with extensive aeolian units in the Blanding Basin and to be N/NE in origin (see Blakey, 1988).

This facieses is interpreted to represent the wettest environment within the Blanding Basin during Lower Sandy/Middle Sandstone time, and it became a trap for suspended sediments as described by Pye (1995). In contrast, within the Rehoboth Member and Upper Sandstone/Salmon Member the Brecciated Sandstone Member is separated from prograding aeolian units in the Blanding Basin by extensive wetter facies (Crinkly Laminated Sandstone) within Sequence II (Carr-Crabaugh and Kocurek, 1998). The positioning of the Brecciated Sandstone Facies distal to prograding aeolian tongues in both cases argues that it represents sediment accumulations on a wetter surface distal to drier sand-sheet environments. Based upon this stratigraphic relationship the euhedral vugs are interpreted as salt-dissolution features and the high concentration of suspended material within the Brecciated Sandstone Facies points toward deposition in an evaporitic sand flat situated between the dune/sand sheets and yet more distal sabkha and shallow subaqueous environments.

FACIES 7: WEAKLY LAMINATED SANDSTONE

The Weakly Laminated Sandstone Facies is expressed as tan to pink, massive, up to 10 m thick strata with weakly visible, laterally discontinuous, sub-centimeter-scale dark-red laminations, best interpreted as resulting from the collapse of salt blisters and cyanobacterial mats (Glennie, 1970; Blakey et al. 1988; Geredes, 2007; Fig. 5G). The sandstone is fine- to very fine-grained with abundant reduction spots and commonly contains randomly located coarse sand grains. This facies contains only 8% by weight grains coarser than 200 μm, and contains a significant amount of suspended load sediments (20%, Fig. 6D).

The Weakly Laminated Sandstone occurs predominantly within the Rehoboth Member of the Blanding Basin, with lesser amounts within the Upper Sandstone/Salmon Member within the Blanding Basin (Fig. 4). The Weakly Laminated Sandstone Facies has its thickest accumulations proximal to the Defiance-Zuni Arch within the Rehoboth Member, and interfingers with Crinkly Laminated Sandstone Facies basinward. Within the Upper Sandstone/Salmon Member, the Weakly Laminated Sandstone Facies is found basinward of Planar-Laminated Sandstone Facies and inter-fingers with Crinkly Laminated Sandstone Facies.

Based on its stratigraphic position in relation to facies of aeolian dune and sand sheet origin and its inter-fingering relationship with Crinkly Laminated Sandstone Facies, along with the presence of cyanobacterial mats, the Weakly Laminated Sandstone Facies is interpreted as an occasionally wetted sabkha deposit distal to sand sheet and salt flat environments.

FACIES 8: CRINKLY LAMINATED SANDSTONE

The Crinkly Laminated Sandstone Facies forms dark-red to pink-colored units composed of abundant, laterally continuous, centimeter-scale laminations of dark-red, silty sand and pink, fine-grained sand (Fig. 5F). Abundant ~ 5 cm long, ~ 2 cm thick lenses of fine-grained sand with cryptic low angle foresets are interpreted as preserved ripple lenses. The ratio of dark-red, crinkly, silty sand laminations to pink, fine-grained laminations varies, with increasing abundance crinkly silty sand laminations corresponding with a more recessive weathering profile. This facies contains a high proportion (35%) of grains finer than 62 µm (Fig. 6E).

The Crinkly Laminated Sandstone Facies comprises the bulk of the Entrada Sandstone within the Blanding Basin, especially within the Rehoboth and Upper

Sandstone/Salmon members, as well as within the San Juan Basin, where the entire Rehoboth Member is composed of Crinkly Laminated Sandstone (Fig. 4). The Crinkly Laminated Sandstone Facies inter-fingers with and superimposes Weakly Laminated Sandstone Facies throughout the Blanding Basin, and completely encases the Todilto Member within the San Juan Basin.

Based on lateral relationships, as well as grain size analysis and the abundance of crinkly silty laminations, interpreted as salt blisters and cyanobacterial mats, the Crinkly Laminated Sandstone Facies is interpreted as frequently wetted sabkha deposit that occurred during wet periods within the study area resulting from either high water table or cyclic wetting from tidal influence.

Idealized Facies Profile and Facies Track

The lateral relationships discussed above correspond with three trends evident in grain size and sedimentary structure analysis: (1) an increase in possible loess fraction basinward, (2) a decrease in sand coarser than 200 μm basinward, and (3) an increase in waterlain sedimentary structures basinward (Figs. 4, 5, 6). Suspended load fraction increases and grain size becomes finer basinward due to down-wind sorting of grains away from the dune field, and this corresponds with an increase in waterlain sedimentary structures as shallow marine processes become dominant over aeolian processes. Lateral facies relationships allow for the construction of an "idealized" facies track and vertical profile, although a complete vertical facies succession does not occur within the study area (Figs. 7, 8).

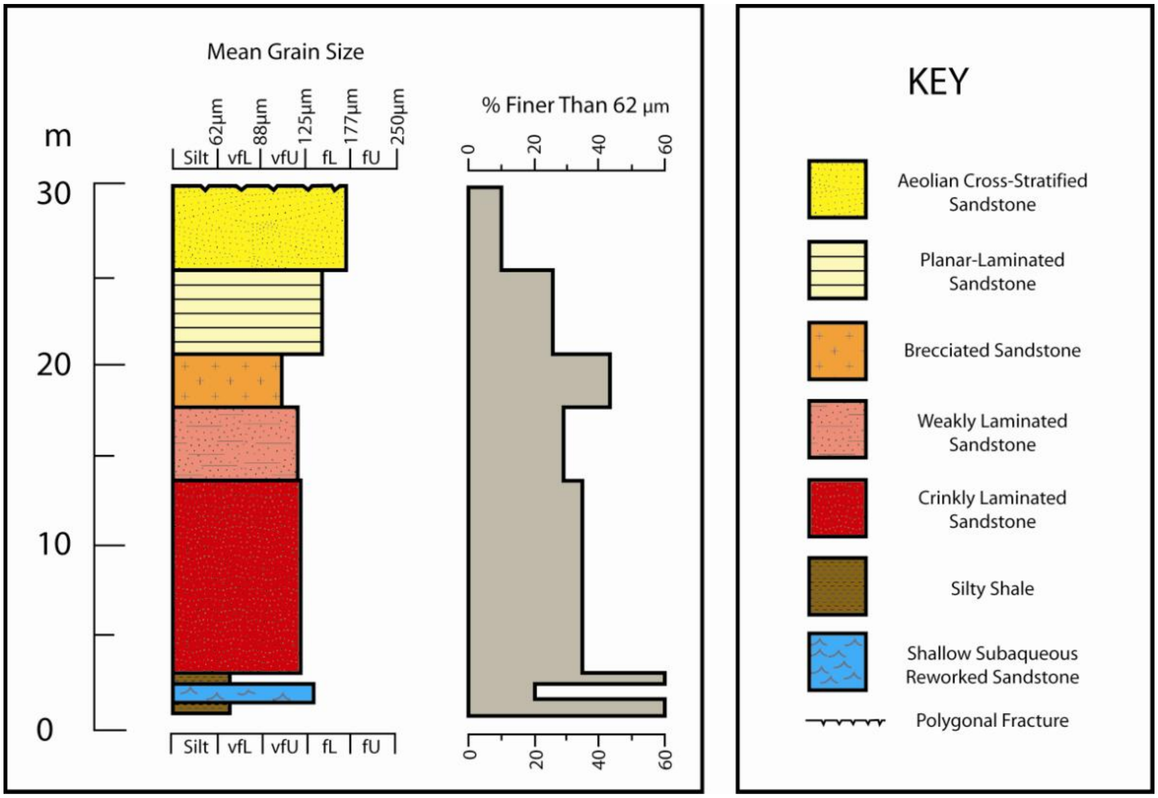

Fig. 7- Idealized vertical profile showing one sabkha and aeolian progradation over shallow marine environments with relative thicknesses for each facies and percent of each facies finer than 62 µm (suspended sediment- or loess-sized grains). Idealized profile created based on facies relationships observed in the field as well as lateral correlations interpreted in Figure 4 and sedimentary analysis displayed in Figure 6.

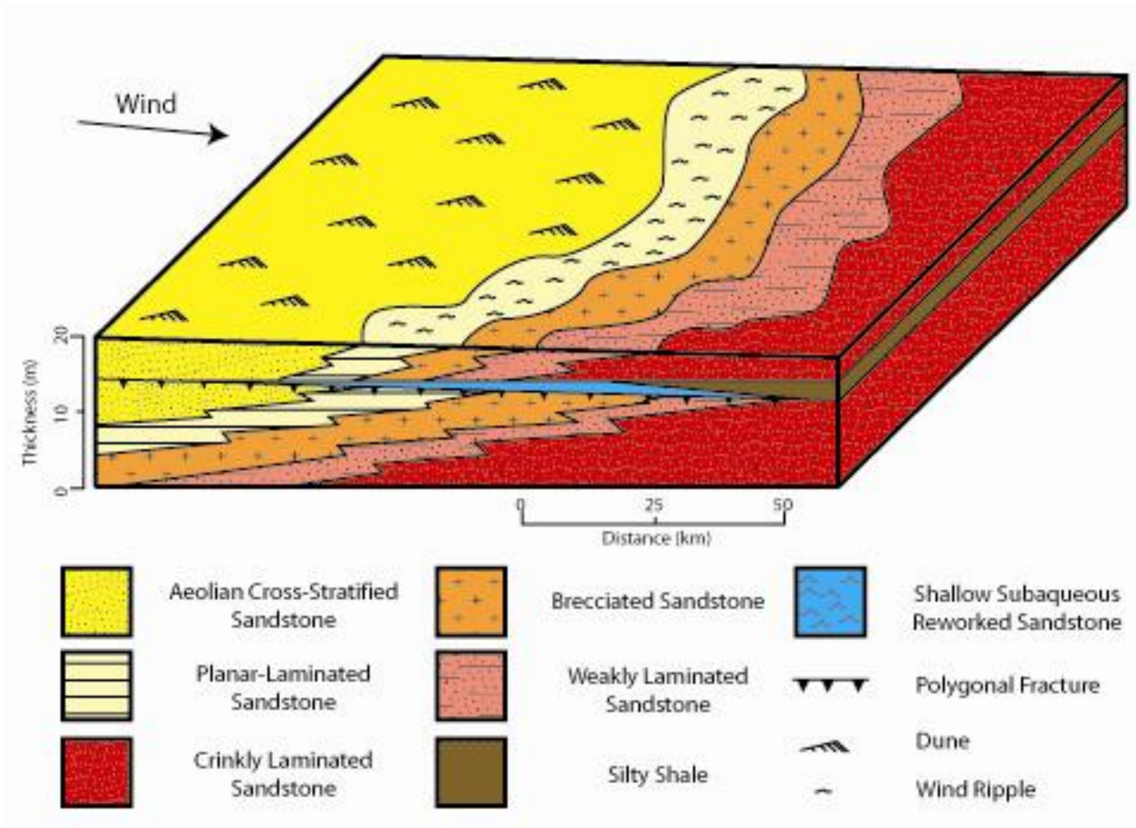

Fig. 8- A facies track diagram showing an idealized progradation of aeolian dune and sand sheet facies over sabkha facies, which is then truncated by a bypass surface marked by polygonal fracture, and transgressed by a marine flooding event and subsequent progradation. Accumulation is governed by a combination of sea level fluctuation and subsidence.

SEQUENCE STRATIGRAPHY

Strata of this study are a continuation of Sequences I and II of Carr-Crabaugh and Kocurek (1998) highlighted in Figure 2. Sequences identified in the former study are evident here and show the response of costal facies to relative sea-level change (Figs. 9, 10). Sequences consist of basal sabkha and shallow marine facies superimposed by progradational aeolian cross-bedded sandstones, which are capped by surfaces of sediment bypass and erosion defined by polygonal fractures (Carr-Crabaugh and Kocurek, 1998; Fig. 10). Accumulation and preservation of aeolian and sabkha sediment is governed by sediment flux, basin subsidence and water table, with a rising water table corresponding to increased accumulation and preservation. In aeolian and sabkha environments proximal to shallow marine environments, water table is largely a function of relative sea-level and serves as its inland proxy. Relative sea level is a function of subsidence, sediment flux, and eustatic sea level. Because there is no independent data on regional subsidence or sediment flux, Carr-Crabaugh and Kocurek (1998) assumed these variables constant in order to constructed a relative sea-level curve from their interpreted sequences (Fig. 9). For this study, we follow this thinking and again assume constant subsidence and sediment flux and allow the water table curve to fluctuate to match the observed sequences.

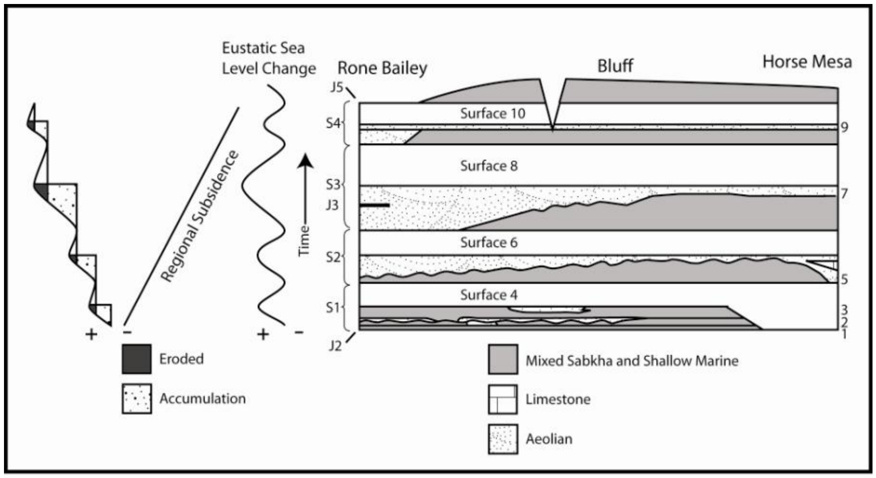

Fig. 9- A modified Wheeler diagram showing basic facies relationships and corresponding sea-level relationships for the San Rafael Group from Rone Baily, in easter Utah, to Horse Mesa, in northwestern New Mexico. Accumulations illustrate basic facies relationships shown in Figure 2. Surfaces 1-10 are surfaces identified by Carr-Crabaugh and Kocurek (1998). Modified after Carr-Crabaugh and Kocurek (1998).

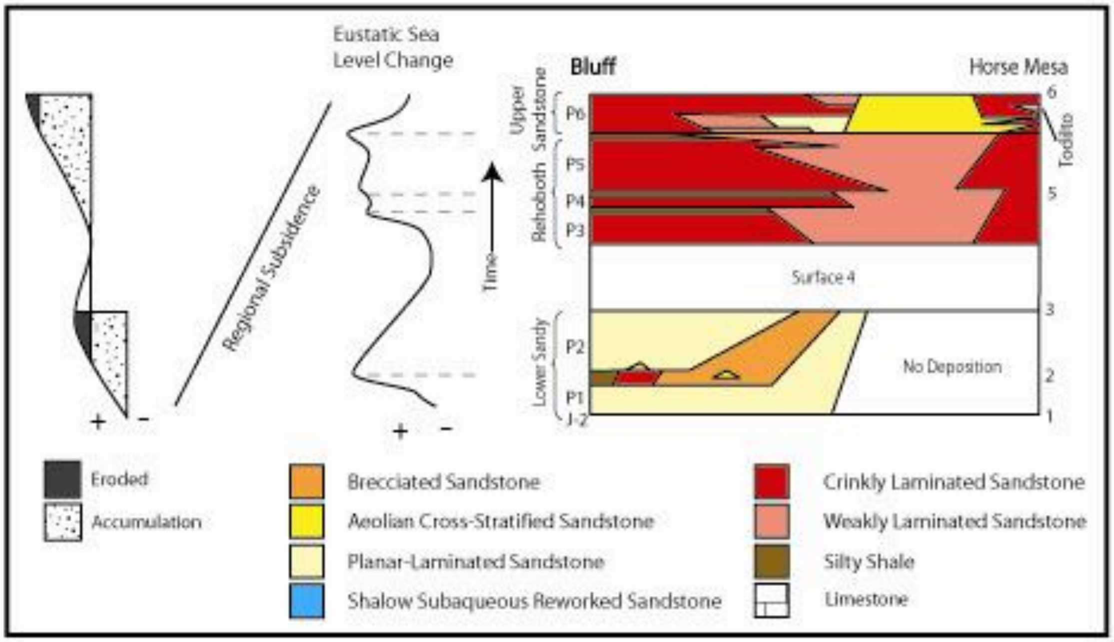

Fig. 10- A modified Wheeler diagram showing facies relationships and corresponding refined sea-level relationships for the Entrada Sandstone from Bluff, Utah, to Horse Mesa, New Mexico. Two sequences identified by Carr-Crabaugh and Kocurek (1998) are traced from the terminus of their study in Bluff, Utah to Horse Mesa, New Mexico, and are subdivided into 6 parasequences. See text for sequence stratigraphic analysis.

Analysis of units in this study allow for a more detailed sea-level curve to be developed for the Entrada Sandstone (Fig. 10). The new curve confirms the general relative sea-level trends established by Carr-Crabaugh and Kocurek (1998), and develops a more detailed understanding of relative sea-level fluctuations based on parasequences within the Entrada. We identify six parasequences, defined by shallow marine transgressions followed by progradation of aeolian dune and sand sheet environments over sabkha and shallow marine environments within the studied zone (Fig. 10).

Lower Sandy Memeber

The Lower Sandy Member (Middle Sandstone Member north of the San Juan River) of the Entrada Sandstone is the aeolian-dominated depositional system of Carr-Crabaugh and Kocurek's "Sequence 1" (Fig. 2). Within the area of this study, the Lower Sandy Member is dominated by Planar-Laminated Sand and Brecciated Sandstone Facies that define two parasequences (P1 and P2) separated by a flooding surface marked by a thin, laterally continuous Silty Shale and Crinkly Laminated Sandstone Facies that transition laterally to Brecciated Sandstone Facies (Figs. 4, 10). Within this member, aeolian cross-stratified sands exist in the distal positions of the area in isolated pods, which represent isolated dunes migrating across the sand sheet as a down-wind representation of better established aeolian dune fields northward (Carr-Crabaugh and Kocurek, 1998) that were driven southward by prevailing northeasterly winds as discussed previously (Blakey, 1988; Parrish and Peterson, 1988). The Lower Sandy Member thickens significantly northward of the Defiance-Zuni Arch, indicating active subsidence within the Blanding Basin during Lower Sandy Member deposition (Kelly, 1955). There is no correlative unit for the Lower Sandy Member within the study area in the San Juan Basin; however, the Middle Sandstone Member is equivalent to the Iyanbito Member of the Entrada Sandstone more distally within the San Juan Basin (Robertson and O'Sullivan, 2000). The Middle Sandstone Member is capped by a polygonally fractured surface across the entire study area where it is present.

Rehoboth Member

The Rehoboth Member is the basal sabkha dominated portion of "Sequence 2" of Carr-Crabaugh and Kocurek (1998; Fig. 2). This member is represented within the southern Blanding Basin by three parasequences (P3-P5) composed of prograding tongues of drier sabkha (Weakly Laminated Sandstone Facies) interfingering with wetter sabkha (Crinkly Laminated Sandstone Facies) and separated by Silty Shale Facies and small amounts of Brecciated Sandstone Facies, which collectively represent a flooding surface (Figs. 4, 10). Within the San Juan Basin and study area the Rehoboth Member sits atop the J2 Unconformity and consists of a thick deposit of wet sabkha. The relatively constant thickness of the Rehoboth Member across the Blanding Basin confirms the interpretation that thickness of this member can be contributed to an increase in the rate of creation of accommodation caused by eustatic sea level rise during Rehoboth time (Carr-Crabaugh and Kocurek, 1998).

Upper Sandstone Member

The Upper Sandstone/Salmon Member is the dune-interdune depositional system capping "Sequence 2" (Carr-Crabaugh and Kocurek, 1998; Fig. 2). Aeolian sands within the Upper Sandstone Member of the San Juan Basin and along the Defiance-Zuni Arch within the southern Blanding Basin have different origins than similar sands found within the Lower Sandy/Middle Sandstone Member, as previously discussed. Aeolian sands within the Upper Sandstone Member were transported to the area from the northeast, not from the north across the Blanding Basin. Within the southern Blanding Basin, this member is composed of an initial progradation marked by aeolian cross-stratified facies on the Defiance-Zuni Arch transitioning basinward into sand flat and dry sabkha facies (Fig. 4). This southwesterly-westerly prograding tongue of aeolian cross-stratified sand, and its distally correlative sand sheet deposits, is then transgressed by wet sabkha facies, marking the last parasequence within the Entrada (P6; Figs. 4, 10).

Within the San Juan Basin, the Upper Sandstone Member is composed of two parasequences marked by progradational tongues of aeolian cross-stratified sands over sand flat deposits separated by wet sabkha deposits (Fig. 4, 10). The second parasequence is transgressed by wet aeolian deposits, within which lies the Todilto Limestone. The upward-wetting trend seen in the Upper Sandstone Member is further evidence supporting the interpretation that the Upper Sandstone Member was deposited during relative sea-level rise as described in Carr-Crabaugh and Kocurek (1998).

Todilto Limestone Member

The Todilto Limestone exists within the San Juan Basin of northeastern New Mexico, and pinches out against the Defiance-Zuni Arch within the eastern margins of the study area (Fig. 4). It was formed as a result of a catastrophic flooding event that covered the Entrada Sandstone of the San Juan Basin with as much as 90 meters of water (Kirkland et al. 1995). The Todilto Limestone is a member of a series of evaporate and evaporitic carbonate facies that has historically been included as the basal member of the

Wanakah Formation, or given formation status but correlated with the Lower Member of the Wanakah Formation in northwestern New Mexico (Wright and Becker, 1951; Anderson and Lucas, 1992), and has been interpreted by others as superimposing the Entrada at the J3 Unconformity (Lucas and Anderson, 1997). Based on the correlative framework of O'Sullivan (1978, 1980), these interpretations correlate the Todilto Limestone, and the catastrophic flooding event that formed it, within the base of the Moab Tongue of the Entrada within the Slick Rock Member (Fig. 2). Sedimentologic analysis and stratigraphic correlations of this study, however, demonstrate that the Todilto Limestone lies stratigraphically within the Upper Sandstone Member of the Entrada Sandstone along the margins of the San Juan Basin in western New Mexico, and not above the Upper Sandstone or within the basal member of the Wanakah formation (Fig. 4). This means that the catastrophic flooding event occurred much earlier during the Curtis Transgression, and that the Todilto Formation correlates well within the lower Slick Rock Member in the Paradox Basin, and not stratigraphically above the J3 Unconformity as previously suggested (Fig. 2).

Several causes for the flooding of the San Juan Basin are possible, including (1) an instantaneous breach that filled the San Juan Basin with no eustatic sea level rise, (2) a breach due to eustatic sea level rise that overtopped a ridge separating the San Juan Basin from open marine environments elsewhere, or (3) groundwater flux within the San Juan Basin with no connection to open marine environments elsewhere. The stratigraphic correlation of the Todilto Limestone within the upper portions of the Upper Sandstone Member of the Entrada Sandstone in the San Juan Basin ties the flooding of the San Juan

Basin to a wetting upward trend within the Blanding Basin that corresponds with a regional rise in relative sea-level. This evidence supports the conclusion that the flooding of the San Juan Basin occurred due to a breach during a regional sea level rise, and that it was not due to local ground water flux. The exact location of the breach that connected the San Juan Basin to open marine environments is unclear, but several possible locations have been suggested (Mckee et al., 1956; Harshbarger et al. 1957; Ridgely, 1977).

CONCLUSIONS

The origins of previously undifferentiated, very fine-grained, red, silty sandstone facies of the Entrada Sandstone within the Four Corners Region are interpreted using a combination of field observations, grain size analysis, and stratigraphic positioning relative to facies of known aeolian dune and shallow subaqueous environments. Correlation of measured sections along an 85 km transect spanning portions of the Blanding and San Juan basins highlights facies relationships which, combined with grain size analysis showing trends in proportions of traction load vs. suspended, lead to the differentiation of 8 facies within the study area: (1) Silty Shale, interpreted as a shallow marine transgressive unit, (2) Shallow Subaqueous Reworked Sandstone, interpreted as shallow marine current and wave reworking of previously deposited sediments, (3) Brecciated Sandstone, interpreted as salt flat deposits, (4) Crinkly Laminated Sandstone, interpreted as wet sabkha, (5) Weakly Laminated Sandstone, interpreted as dry sabkha, (6) Planar-Laminated Sandstone, interpreted as sand sheet deposits, (7) Cross-Stratified Sandstone, interpreted as aeolian dune deposits, and (8) Micritic Limestone, which represents the catastrophic flooding of the San Juan Basin.

Sequence stratigraphic analysis using the facies framework developed in this study builds on previous work by Carr-Crabaugh and Kocurek (1998) and increases the detail of understanding of relative sea-level fluctuations within the Blanding and San Juan Basins during Entrada deposition, defining six parasequences within two previously identified sequences. This analysis supports the conclusion that the Entrada Sandstone was deposited as a wet aeolian system during a regional rise in relative sea-level.

The Todilto Limestone pinches out within the Upper Sandstone Member of the Entrada Sandstone within the San Juan Basin and correlates with a relative sea-level rise evidenced in the upper portions of the Salmon/Upper Sandstone Member within the Blanding Basin by a wetting upward cycle marked by Crinkly Laminated Sandstone Facies (frequently wet sabkha) superimposing Weakly Laminated Sandstone (occasionally wet sabkha) and Planar-Laminated Sandstone (sand sheet) Facies. This correlation establishes that the flooding of the San Juan Basin corresponds with a regional sea-level rise, thereby supporting the theory that the catastrophic flooding of the San Juan Basin occurred due to a breach caused by high sea-level. Also, this correlation demonstrates that the Todilto Limestone correlates with the Slick Rock Member of the Entrada Sandstone and not positioned above the J2 Unconformity as proposed by Wright and Becker (1951), Anderson and Lucas (1992), and Lucas and Anderson (1997).

APPENDIX 1: STATISTICAL ANALYSIS OF GRAIN SIZE DATA

Statistical Analysis of Coarse Fraction (>32 µm)

	Aeolian X-Stratified	Planar Laminated	Brecciated	Weakly Laminated	Crinkly Laminated
x̄ (µm)	151	129	106	113	113
Median (µm)	144	124	99	111	113
Mode (µm)	111-120	111-120	86-94	102-111	111-120
Sd (phi)	0.62 Mod Well Std.	0.60 Mod Well Std.	0.59 Mod Well Std.	0.60 Mod Well Std.	0.53 Mod Well Std.
K	0.82 (Platykurtic)	0.89 (Platykurtic)	1.22 (Leptokurtic)	1.05 (Mesokurtic)	1.15 (Leptokurtic)
S	-0.07 (Near Symmetric)	-0.11 (Negative Skewed)	-0.28 (Negative Skewed)	-0.09 (Near Symmetric)	-0.36 (Strongly Negative Skewed)

Statistical Analysis of Total Fraction

	Aeolian X-Stratified	Planar Laminated	Brecciated	Weakly Laminated	Crinkly Laminated
x̄ (µm)	134	102	* 63	* 80	* 77
Median (µm)	134	* 112	* 66	* 99	* 95
Mode (µm)	111-120 <32	111-120 <32	86-94 <32	102-111 <32	111-20 <32
Sd (phi)	0.90 Moderate Std	* 0.99 Moderate Std.	* 0.90 Moderate Std.	* 0.91 Moderate Std.	* 0.96 Moderate Std.
K	16.60 (Extremely Leptokurtic)	* 1.23 (Leptokurtic)	* 1.29 (Leptokurtic)	* 1.16 (Leptokurtic)	0.54 (Very Platykurtic)
S	0.14 (Positive Skewed)	* 0.13 (Near Symmetric)	* -0.11 (Negative Skewed)	* 0.22 (Positive Skewed)	* 0.29 (Positive Skewed)

* Calculations affected by incomplete data within fraction <32µm.

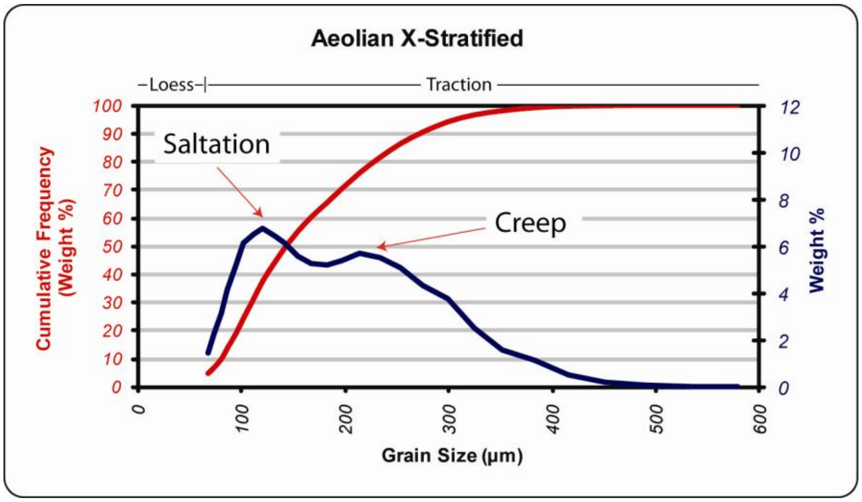
Aeolian X-Stratified
Loess
Traction
Saltation
Creep
Cumulative Frequency (Weight %)
Weight %
Grain Size (µm)
0
100
200
300
400
500
600
10
20
30
40
50
60
70
80
90
2
4
6
8
12

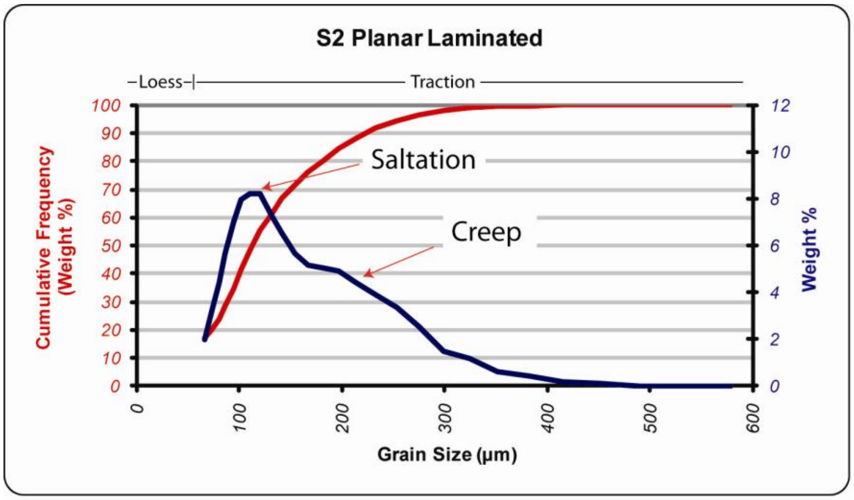
S2 Planar Laminated
-Loess-|
Traction
Saltation
Creep
Cumulative Frequency (Weight %)
Weight %
Grain Size (µm)

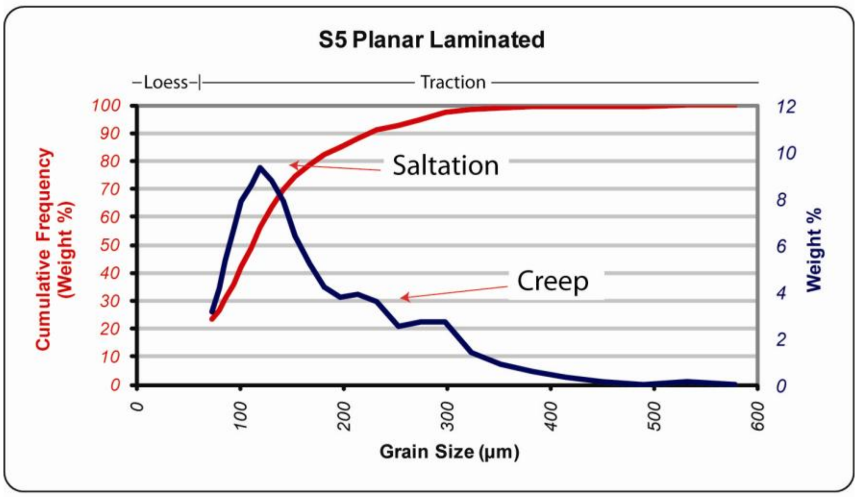
S5 Planar Laminated
-Loess-|
Traction
Saltation
Creep
Cumulative Frequency (Weight %)
Weight %
Grain Size (µm)

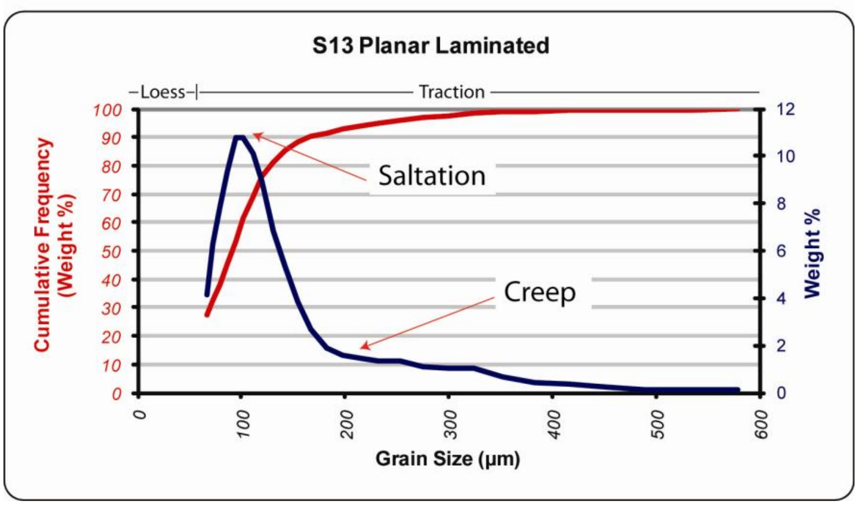
S13 Planar Laminated
-Loess-|
Traction
Saltation
Creep
Cumulative Frequency (Weight %)
Weight %
Grain Size (µm)

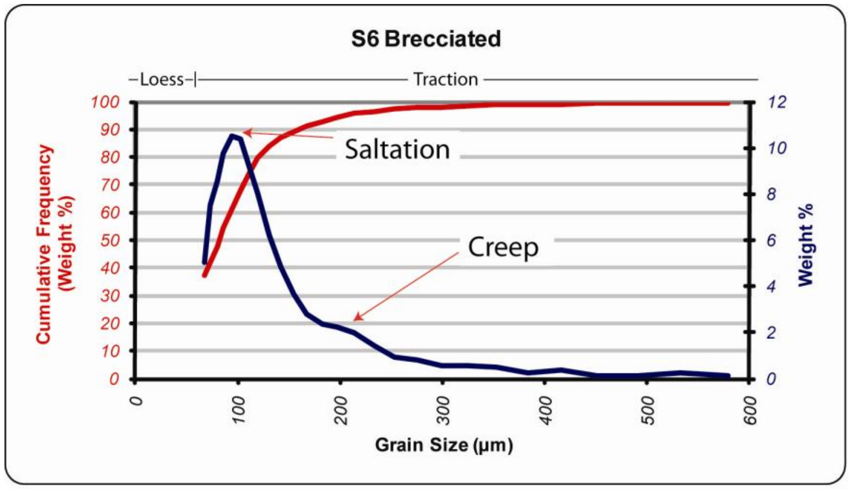
S6 Brecciated
Loess
Traction
Saltation
Creep
Cumulative Frequency (Weight %)
Weight %
Grain Size (μm)

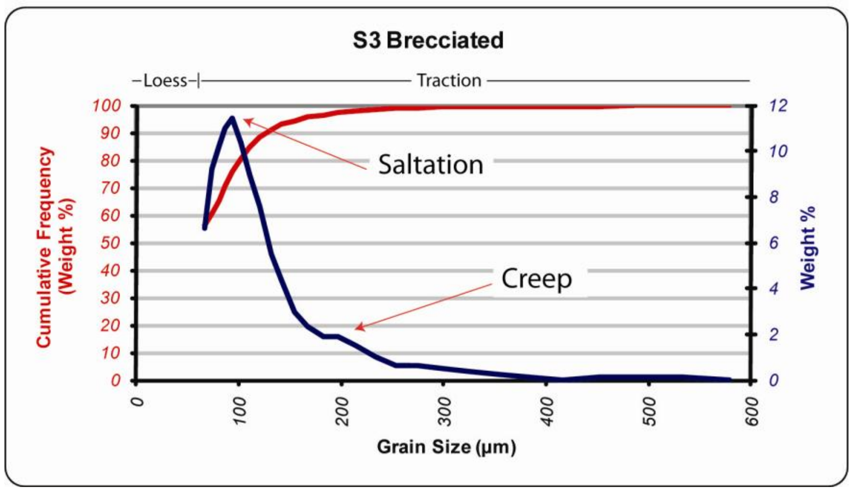
S3 Brecciated
Loess
Traction
Saltation
Creep
Cumulative Frequency (Weight %)
Weight %
Grain Size (μm)

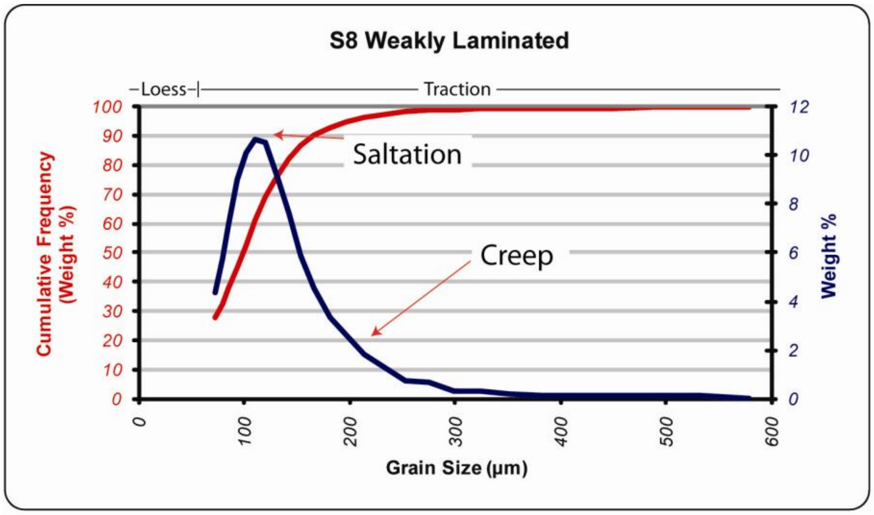
S8 Weakly Laminated
Loess
Traction
Saltation
Creep
Cumulative Frequency (Weight %)
Weight %
Grain Size (µm)
100
90
80
70
60
50
40
30
20
10
0
12
10
8
6
4
2
0
0
100
200
300
400
500
600

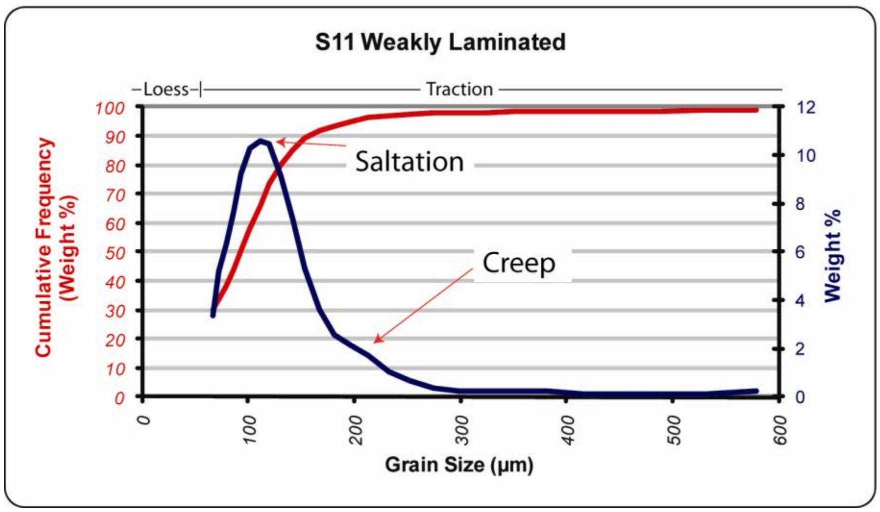
S11 Weakly Laminated
Loess
Traction
Saltation
Creep
Cumulative Frequency (Weight %)
Weight %
Grain Size (µm)
100
90
80
70
60
50
40
30
20
10
0
12
10
8
6
4
2
0
0
100
200
300
400
500
600

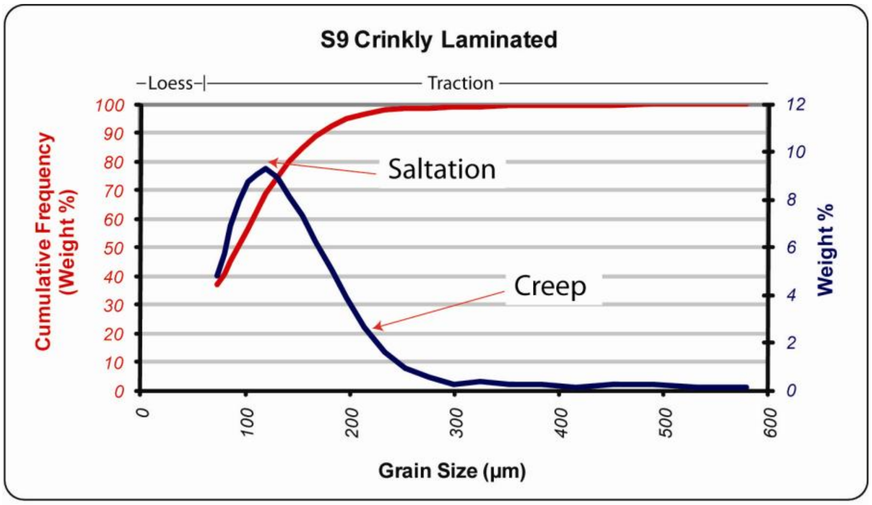
S9 Crinkly Laminated
Loess
Traction
Saltation
Creep
Cumulative Frequency (Weight %)
Weight %
Grain Size (µm)
0
100
200
300
400
500
600

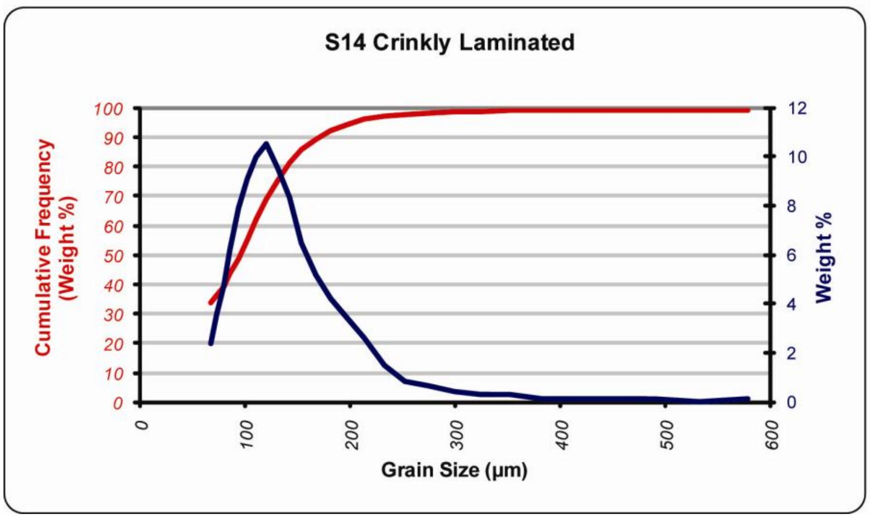
S14 Crinkly Laminated
Cumulative Frequency (Weight %)
Weight %
Grain Size (µm)
0
100
200
300
400
500
600

APPENDIX 2: MEASURED SECTIONS

No.	Section Name	Longitude	Latitude
1	Horse Mesa South	109°03'10"W.	36°40'57"N.
2	Horse Mesa North	109°03'05"W.	36°41'37"N.
3	Beclabito Dome	109°00'26"W.	36°48'09"N.
4	Carrizo West	109°18'03"W.	36°46'44"N.
5	Emanual Mission East	109°22'16"W.	36°47'06"N.
6	Emanual Mission West	109°23'05"W.	36°46'55"N.
7	Sweetwater Mesa East	109°25'58"W.	36°48'20"N.
8	Sweetwater Mesa West	109°28'48"W.	36°51'18"N.
9	Red Mesa East	109°16'55"W.	36°58'52"N.
10	Red Mesa West	109°20'45"W.	36°59'20"N.
11	Mexican Water	109°35'55"W.	36°58'54"N.
12	Tohonadla	109°30'14"W.	37°09'12"N.
13	White Rock Point	109°36'41"W.	37°14'00"N.
14	Butler Wash South	109°38'19"W.	37°16'33"N.
15	Garnet Ridge	109°50'02"W.	36°54'35"N.
16	Red Point	109°55'48"W.	36°47'24"N.
17	Red Point Mesa	109°54'51"W.	36°44'42"N.
18	White Top Mesa North	109°49'08"W.	36°34'55"N.
19	White Top Mesa	109°51'04"W.	36°30'46"N.
20	White Top Mesa South	109°52'33"W.	36°28'27"N.
21	White Top Mesa Southwest	109°55'41"W.	36°28'28"N.
22	White Hills	109°44'31"W.	36°25'44"N.
23	Lohali Point	109°47'51"W.	36°06'51"N.

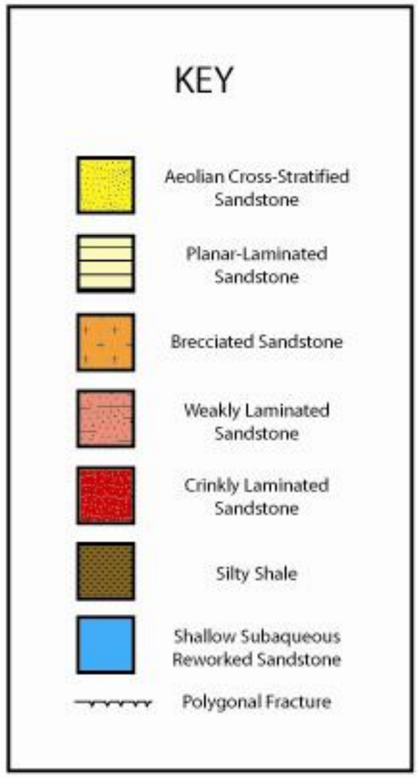
KEY
Aeolian Cross-Stratified Sandstone
Planar-Laminated Sandstone
Brecciated Sandstone
Weakly Laminated Sandstone
Crinkly Laminated Sandstone
Silty Shale
Shallow Subaqueous Reworked Sandstone
Polygonal Fracture

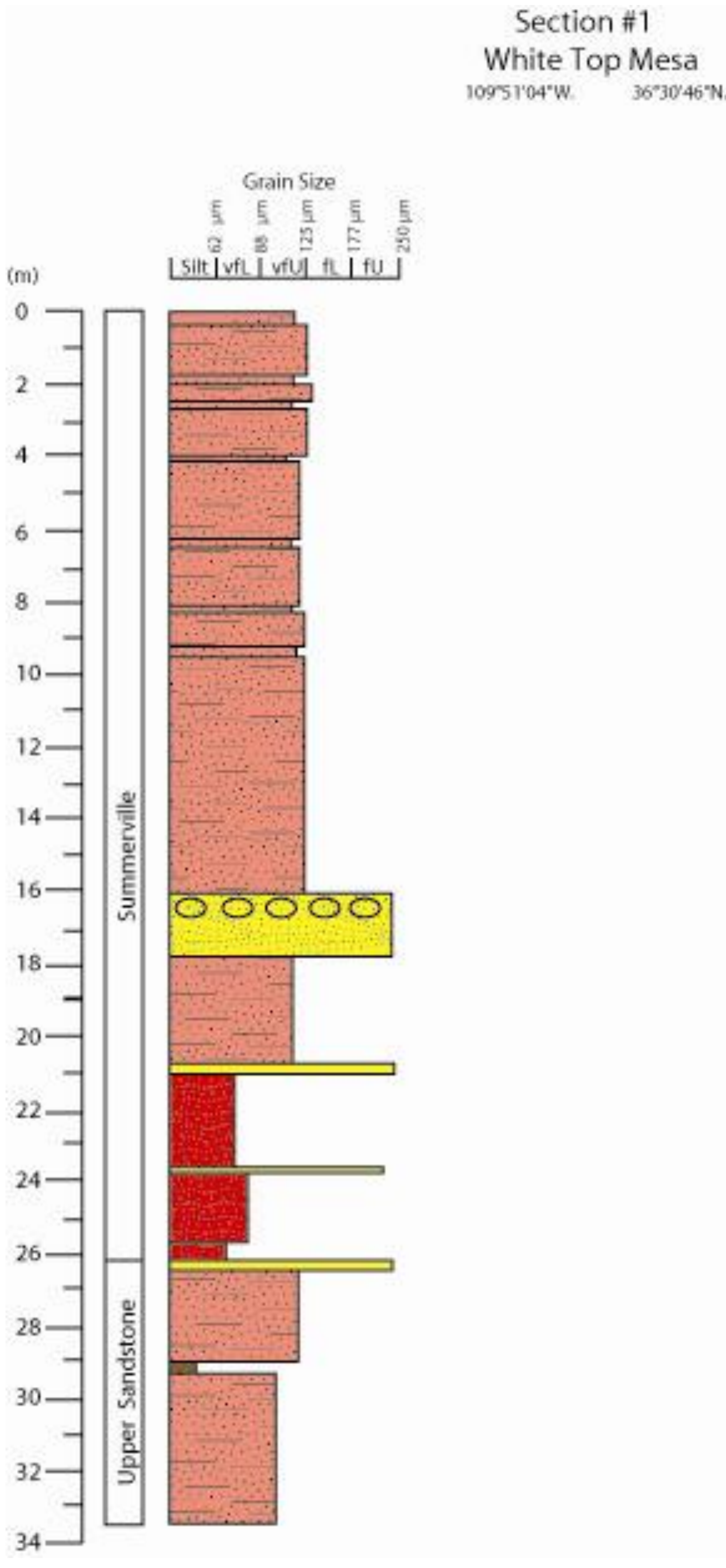
Section #1
White Top Mesa
109°51'04"W. 36°30'46"N.
Grain Size
62 µm
88 µm
125 µm
177 µm
250 µm
Silt
vfL
vfU
fL
fU
(m)
0
2
4
6
8
10
12
14
16
18
20
22
24
26
28
30
32
34
Summerville
Upper Sandstone

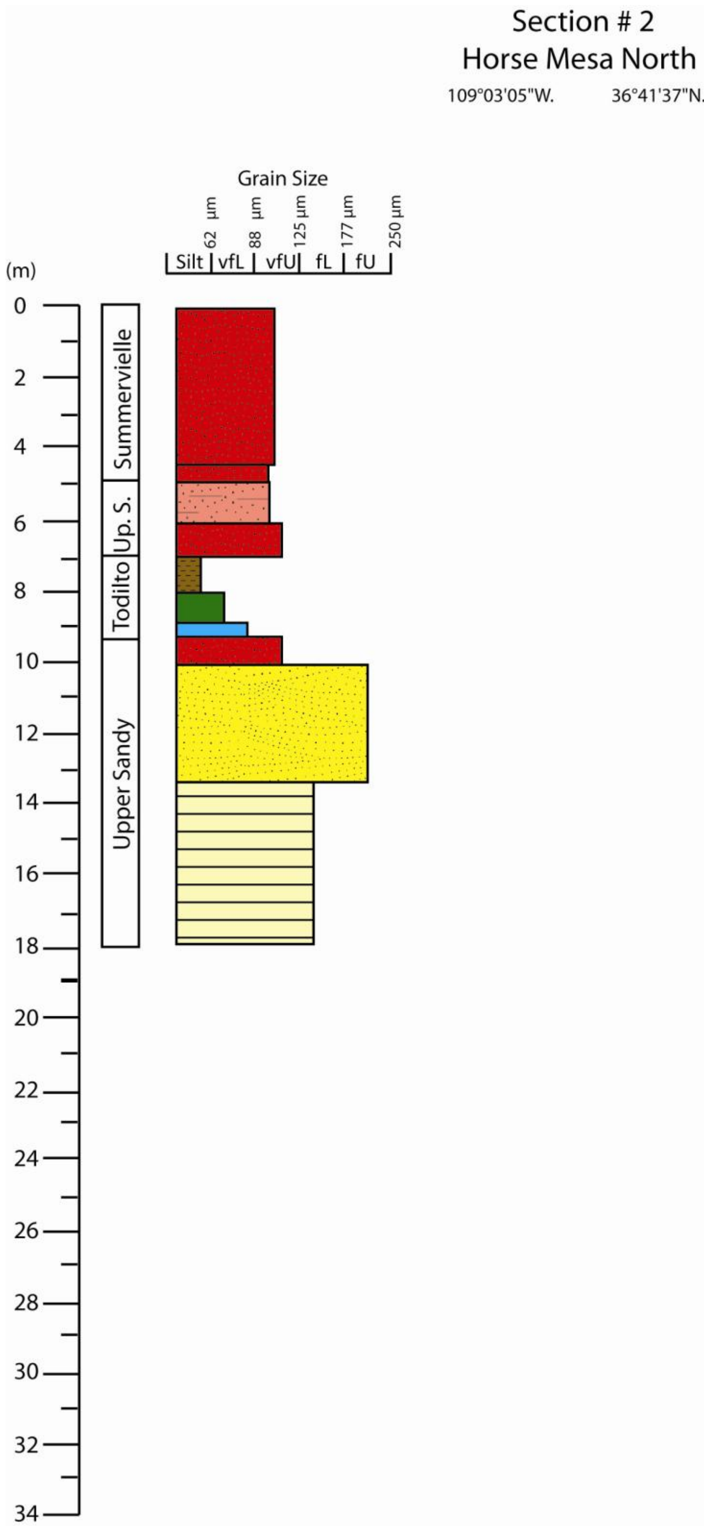
Section # 2
Horse Mesa North
109°03'05"W.
36°41'37"N.
Grain Size
62 µm
88 µm
125 µm
177 µm
250 µm
Silt
vfL
vfU
fL
fU
(m)
0
2
4
6
8
10
12
14
16
18
20
22
24
26
28
30
32
34
Summervielle
Up. S.
Todilto
Upper Sandy

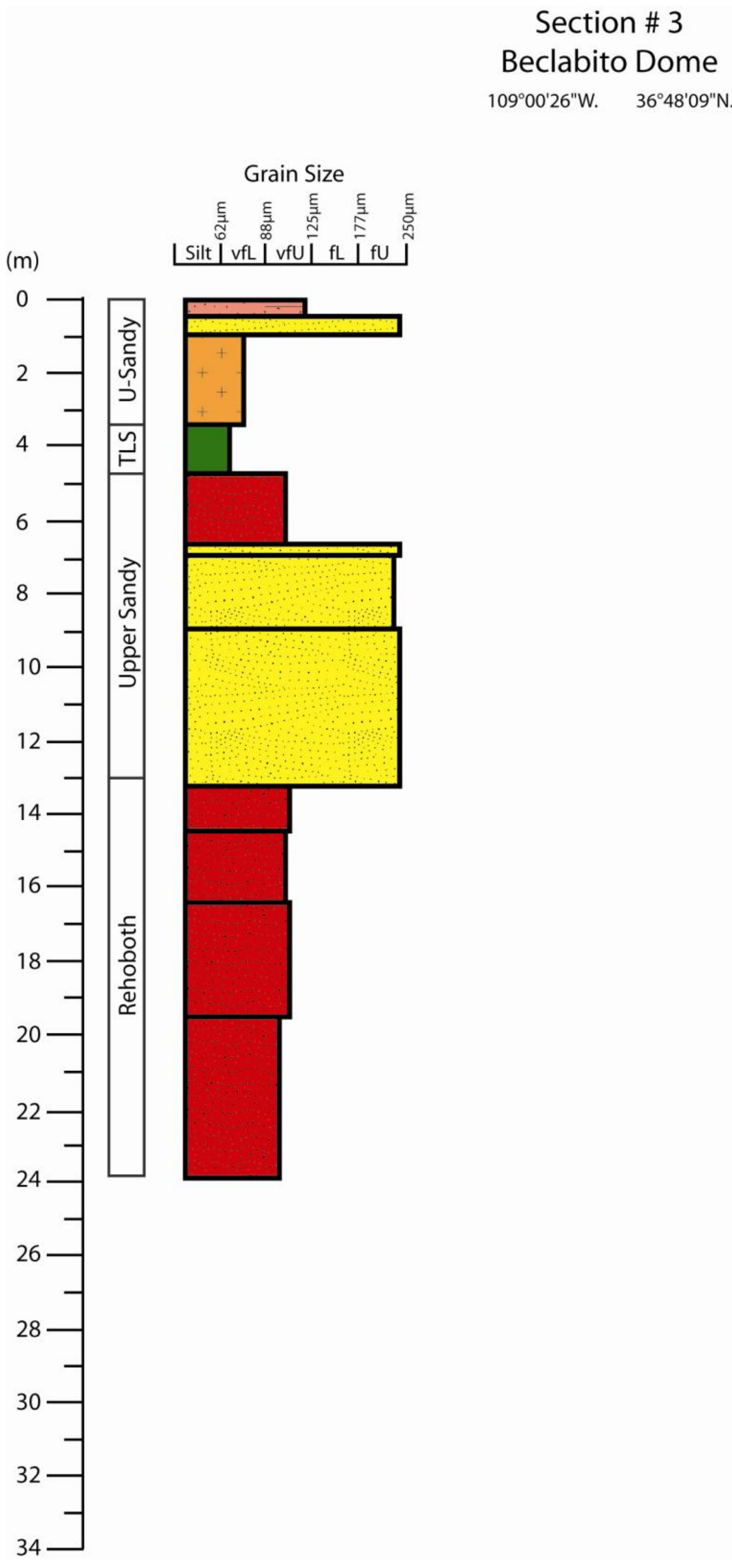

Section # 3
Beclabito Dome
109°00'26"W. 36°48'09"N.
Grain Size
62µm
88µm
125µm
177µm
250µm
Silt
vfL
vfU
fL
fU
(m)
0
2
4
6
8
10
12
14
16
18
20
22
24
26
28
30
32
34
U-Sandy
TLS
Upper Sandy
Rehoboth

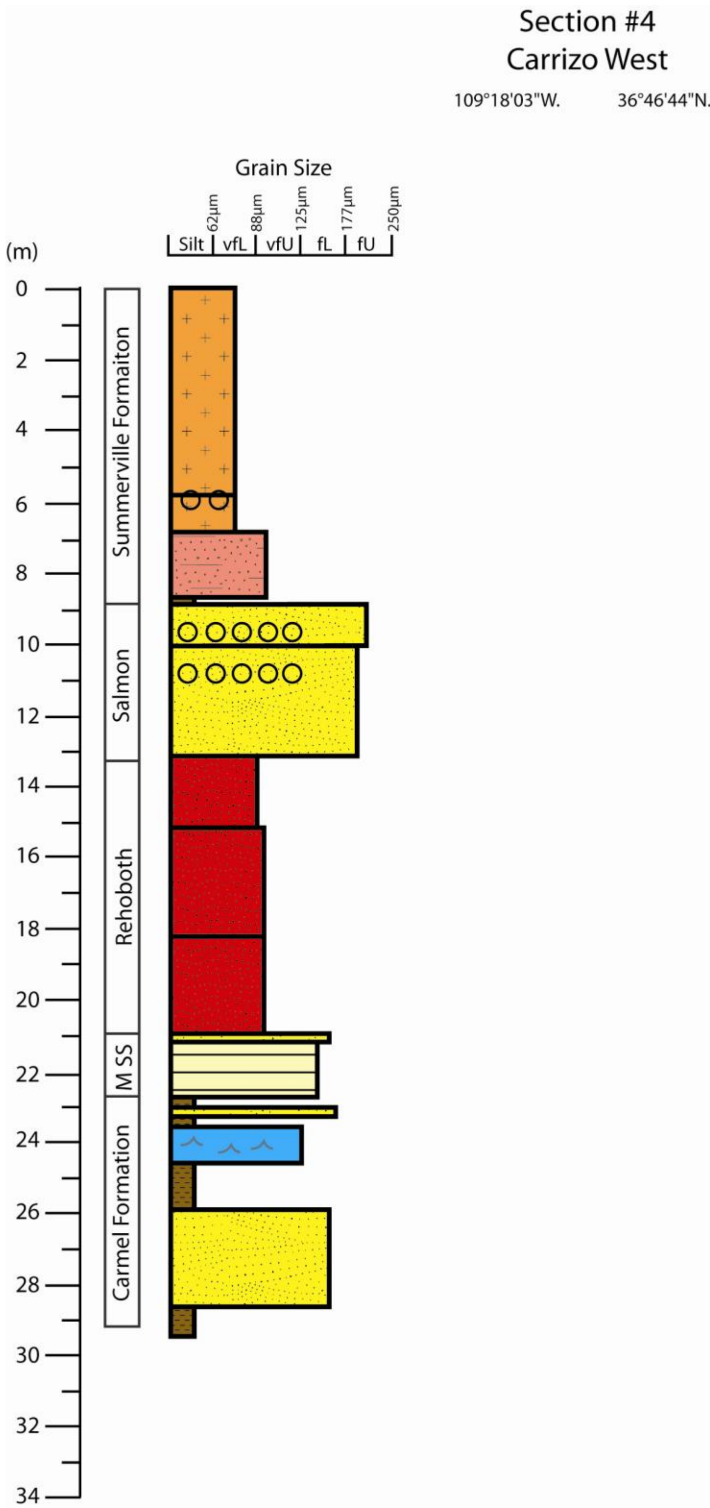
Section #4
Carrizo West
109°18'03"W.
36°46'44"N.
Grain Size
62µm
88µm
125µm
177µm
250µm
Silt
vfL
vfU
fL
fU
(m)
0
2
4
6
8
10
12
14
16
18
20
22
24
26
28
30
32
34
Summerville Formaiton
Salmon
Rehoboth
M SS
Carmel Formation

Section # 5
Emanuel Mission East

109°25'58"W. 36°48'20"N.

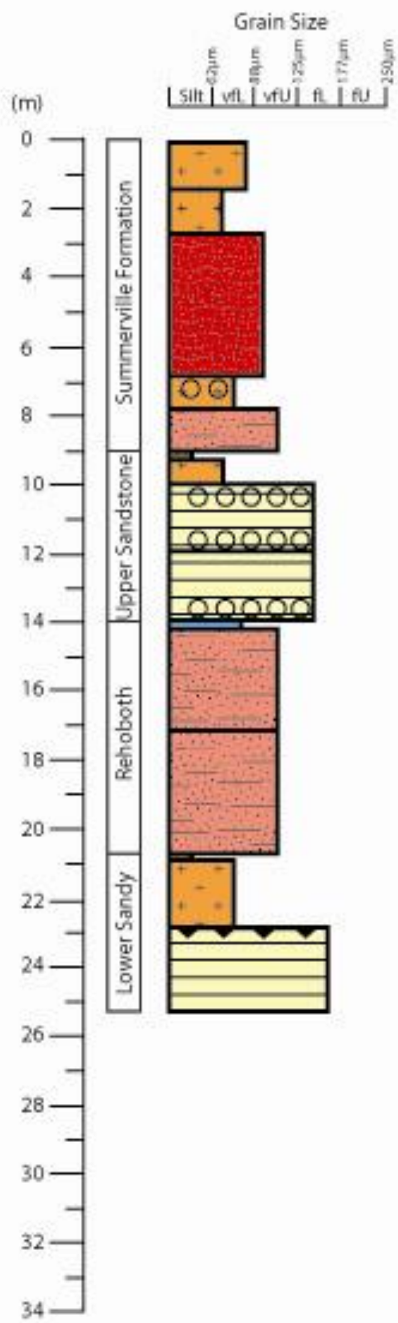

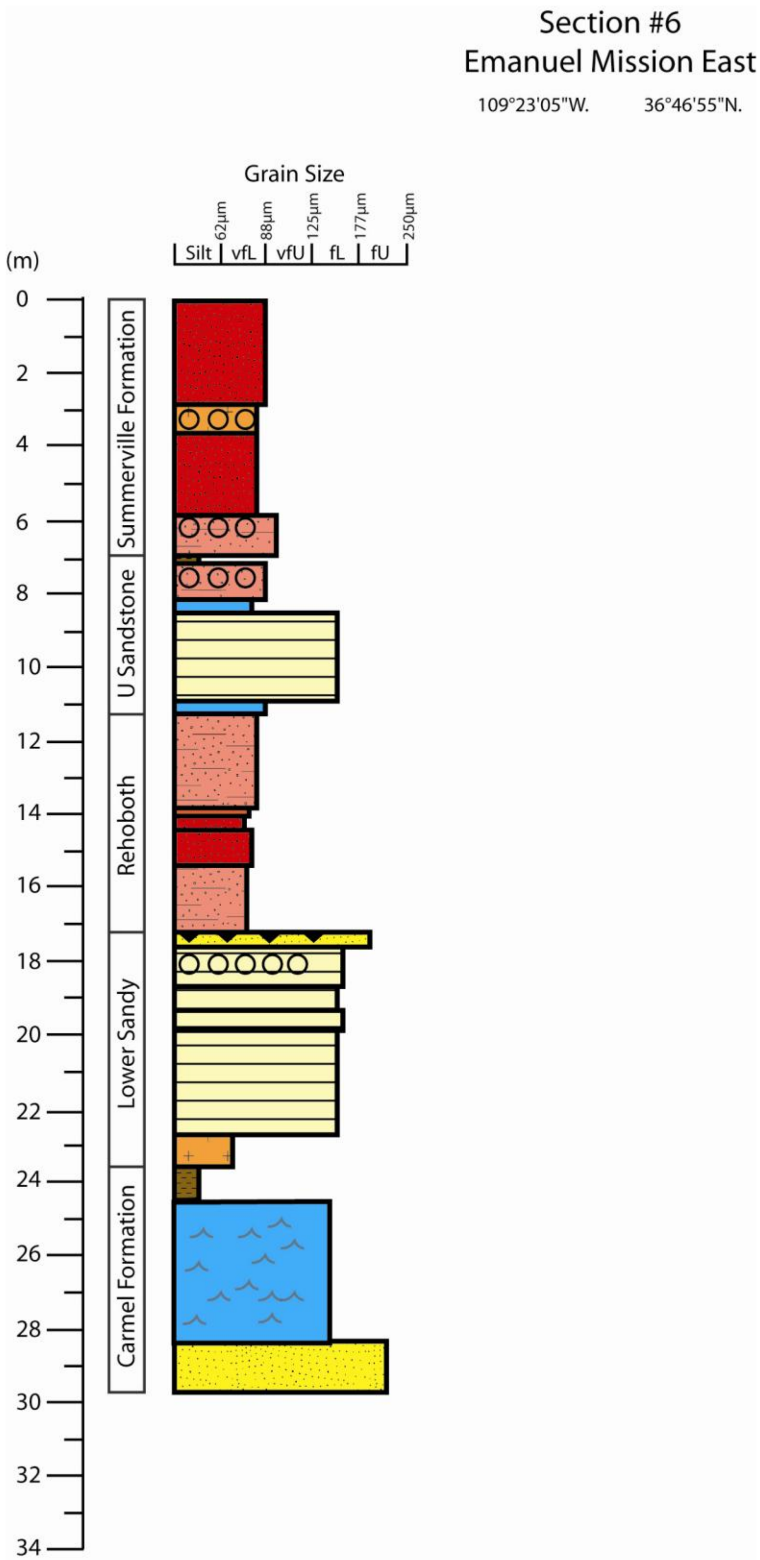
Section #6
Emanuel Mission East
109°23'05"W.
36°46'55"N.
Grain Size
62µm
88µm
125µm
177µm
250µm
Silt
vfL
vfU
fL
fU
(m)
0
2
4
6
8
10
12
14
16
18
20
22
24
26
28
30
32
34
Summerville Formation
U Sandstone
Rehoboth
Lower Sandy
Carmel Formation

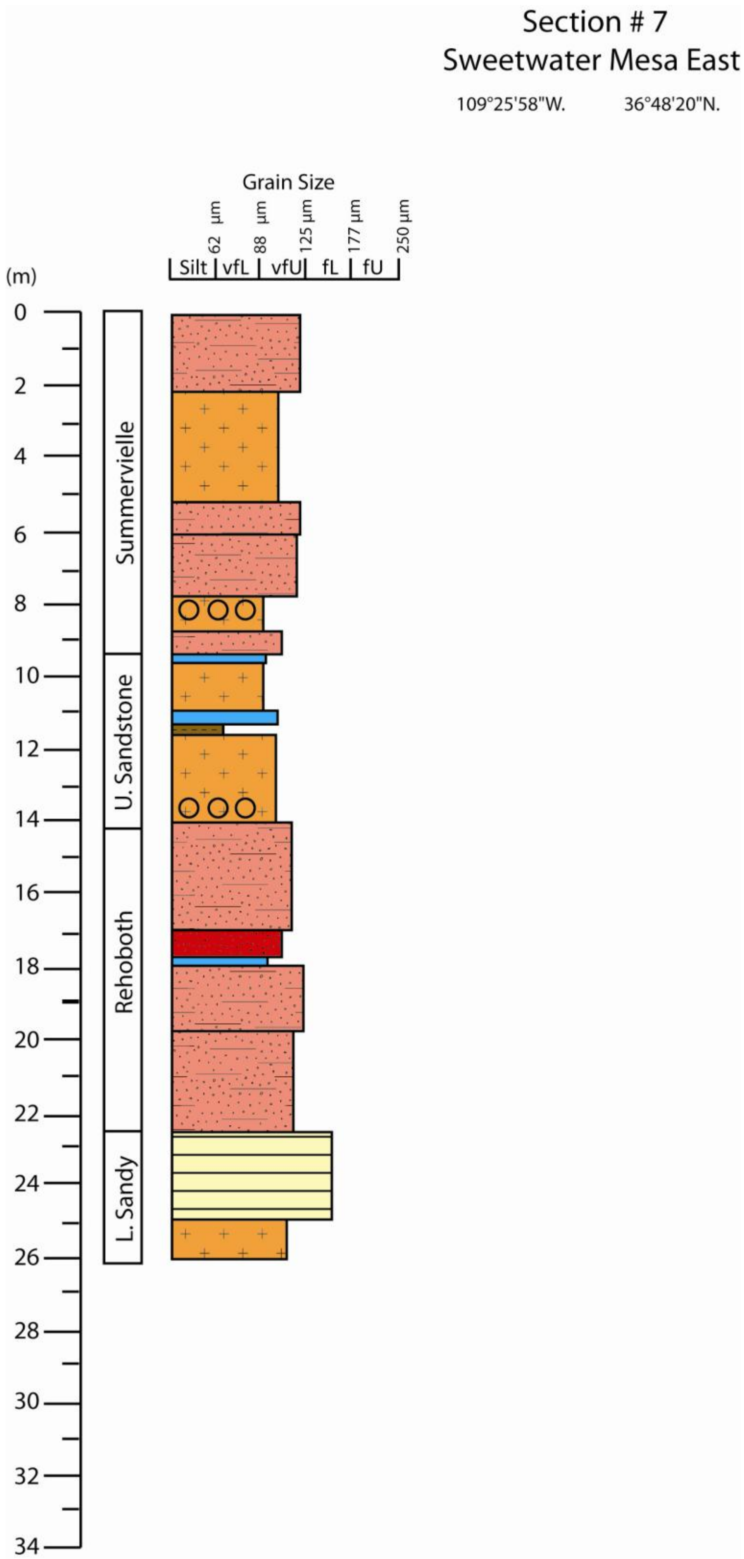
Section # 7
Sweetwater Mesa East
109°25'58"W. 36°48'20"N.
Grain Size
62 µm
88 µm
125 µm
177 µm
250 µm
Silt
vfL
vfU
fL
fU
(m)
0
2
4
6
8
10
12
14
16
18
20
22
24
26
28
30
32
34
Summervielle
U. Sandstone
Rehoboth
L. Sandy

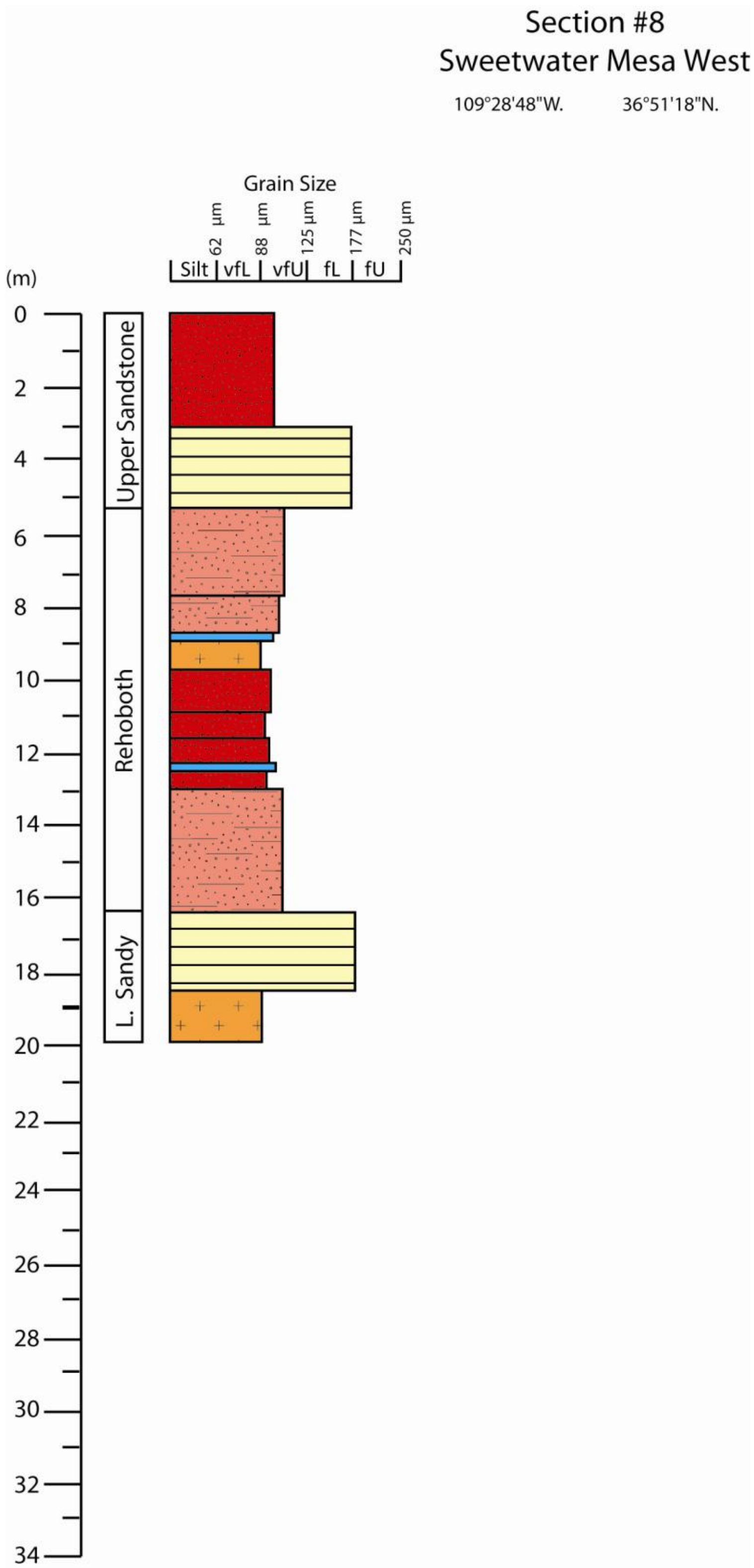
Section #8
Sweetwater Mesa West
109°28'48"W.
36°51'18"N.
Grain Size
62 µm
88 µm
125 µm
177 µm
250 µm
Silt
vfL
vfU
fL
fU
(m)
0
2
4
6
8
10
12
14
16
18
20
22
24
26
28
30
32
34
Upper Sandstone
Rehoboth
L. Sandy

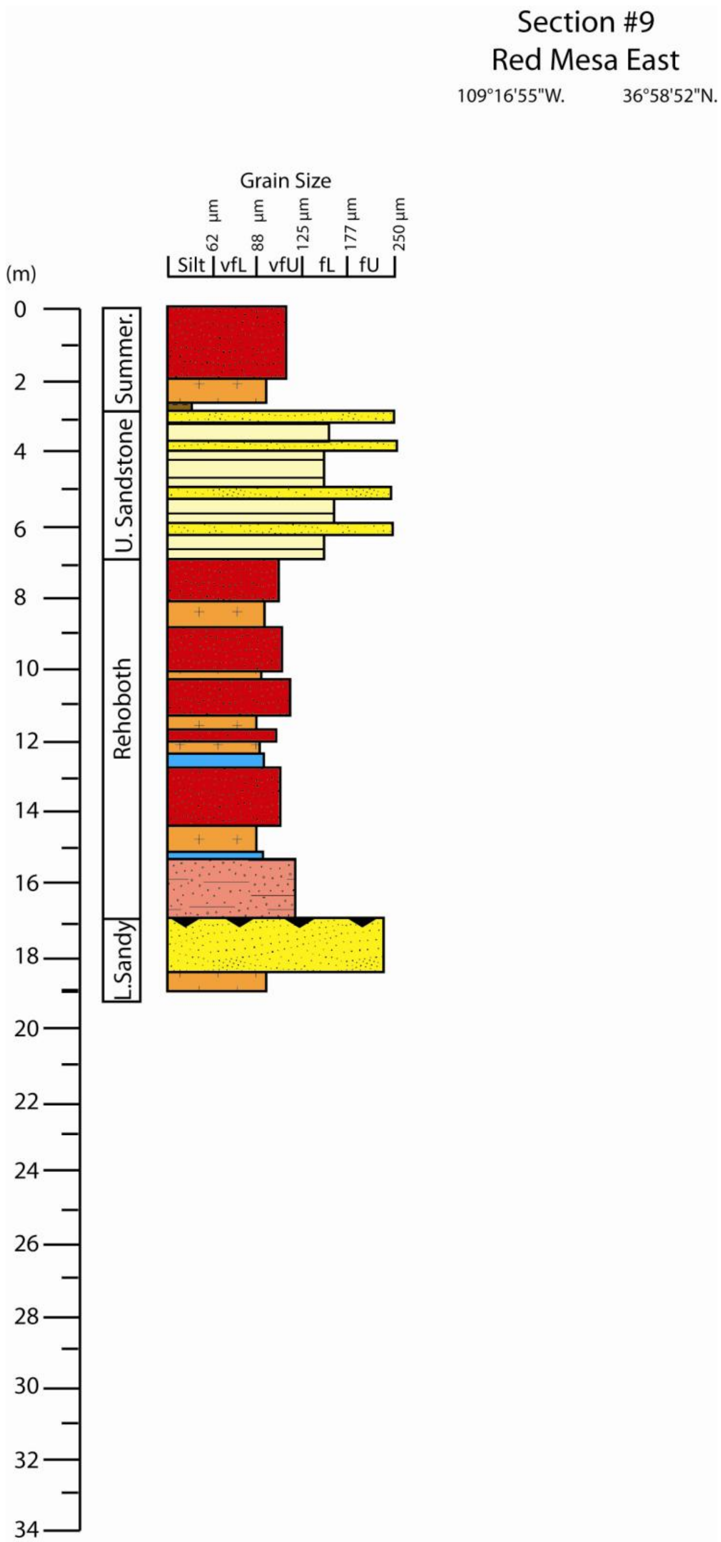

Section #9
Red Mesa East
109°16'55"W.
36°58'52"N.
Grain Size
62 µm
88 µm
125 µm
177 µm
250 µm
Silt
vfL
vfU
fL
fU
(m)
0
2
4
6
8
10
12
14
16
18
20
22
24
26
28
30
32
34
Summer.
U. Sandstone
Rehoboth
L.Sandy

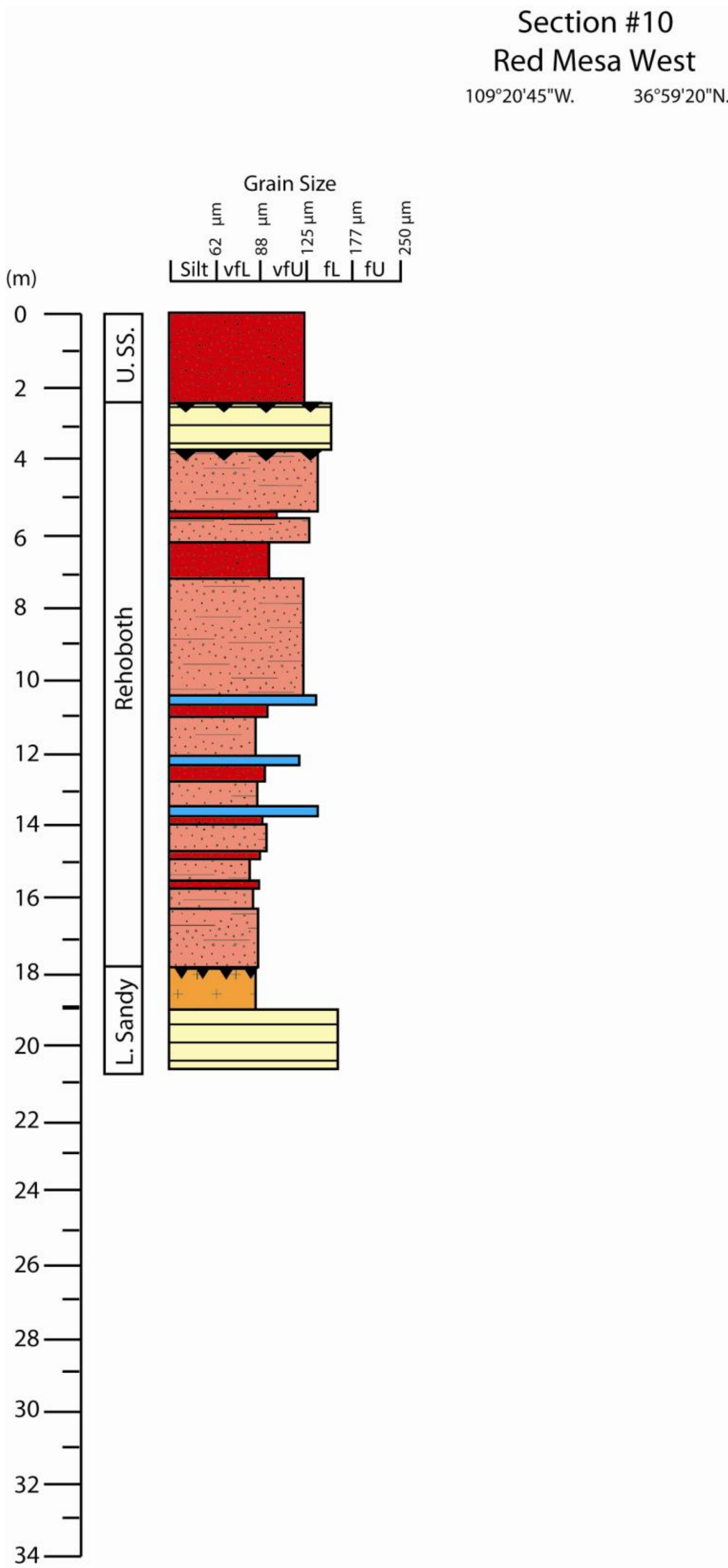

Section #10
Red Mesa West
109°20'45"W.
36°59'20"N.
Grain Size
62 µm
88 µm
125 µm
177 µm
250 µm
Silt
vfL
vfU
fL
fU
(m)
0
2
4
6
8
10
12
14
16
18
20
22
24
26
28
30
32
34
U. SS.
Rehoboth
L. Sandy

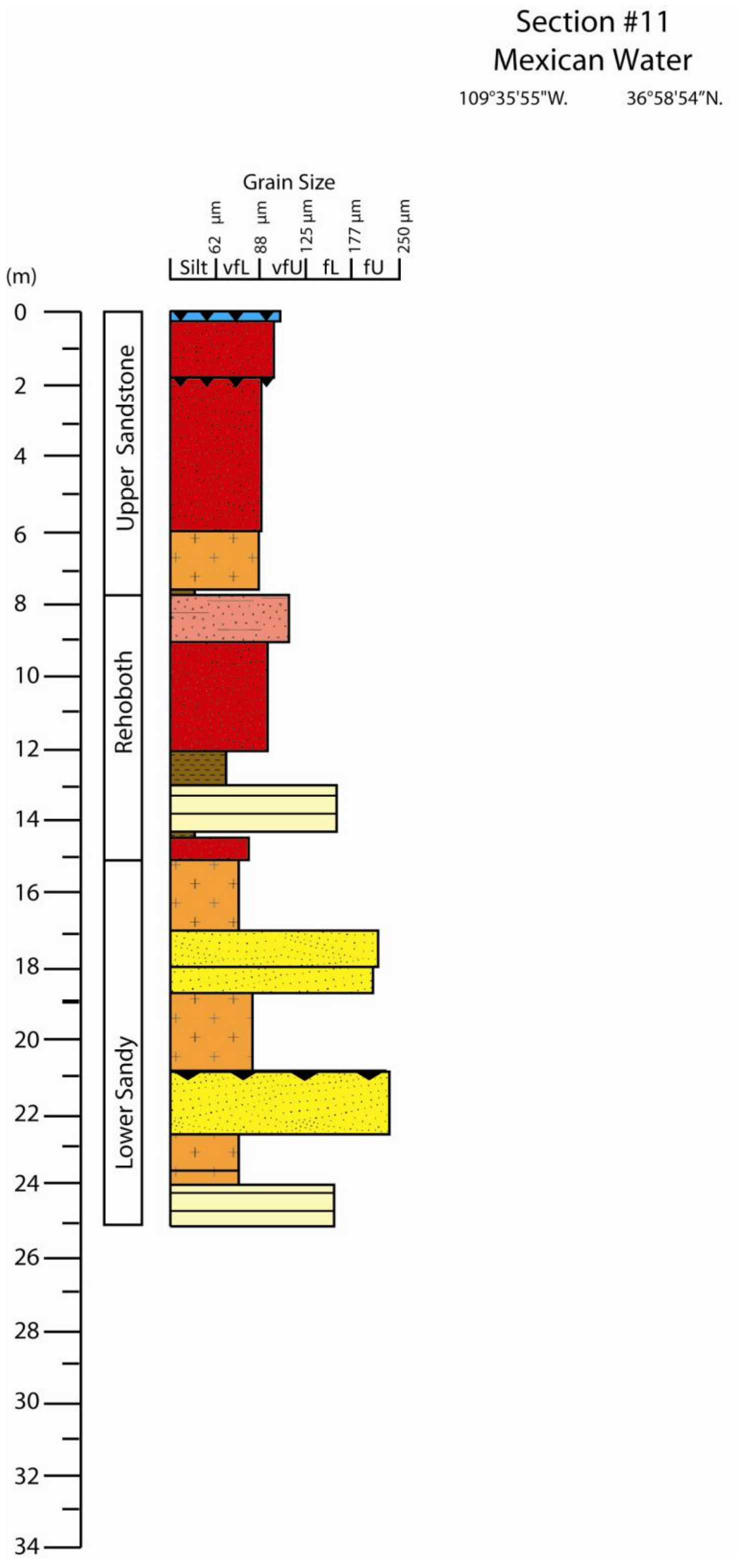
Section #11
Mexican Water
109°35'55"W.
36°58'54"N.
Grain Size
62 µm
88 µm
125 µm
177 µm
250 µm
Silt
vfL
vfU
fL
fU
(m)
0
2
4
6
8
10
12
14
16
18
20
22
24
26
28
30
32
34
Upper Sandstone
Rehoboth
Lower Sandy

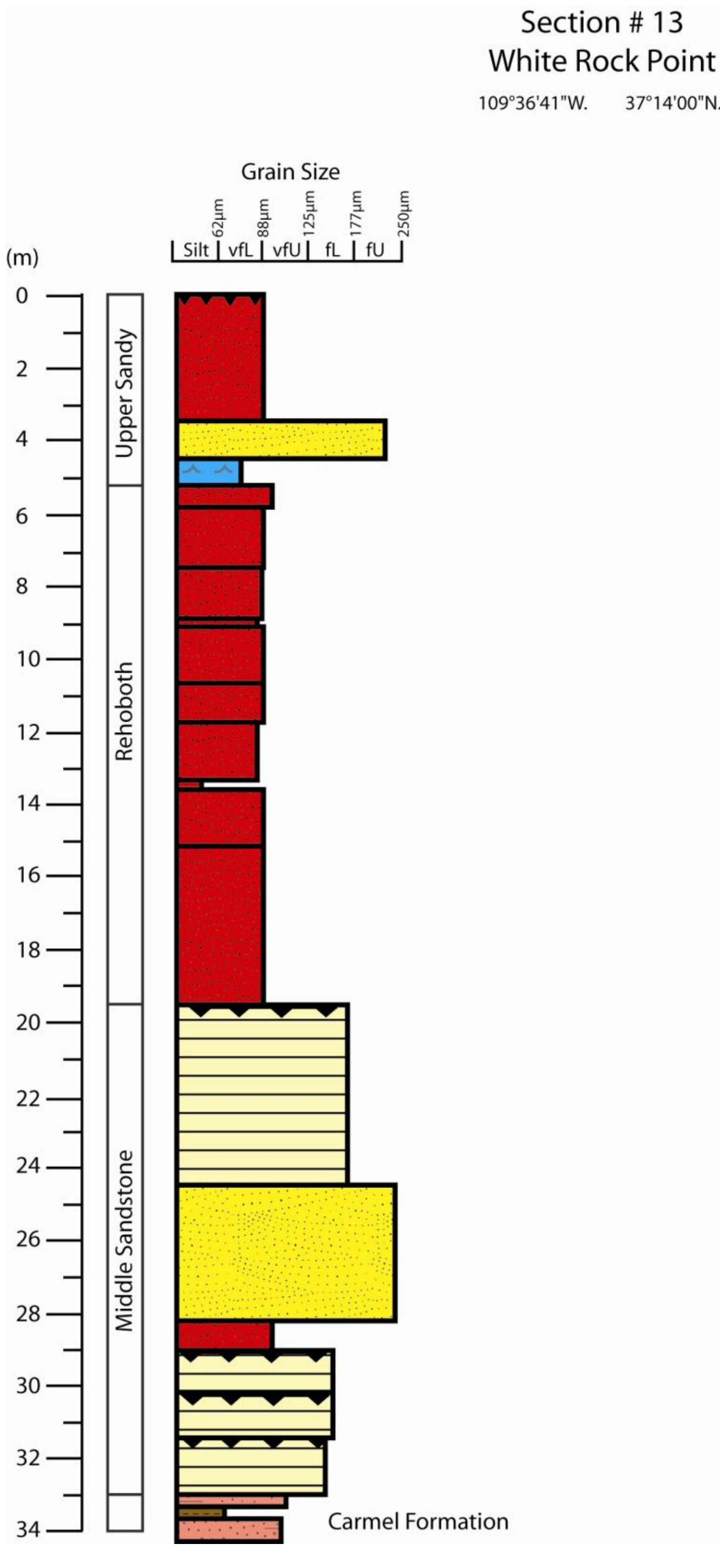
Section # 13
White Rock Point
109°36'41"W. 37°14'00"N.
Grain Size
62µm
88µm
125µm
177µm
250µm
Silt
vfL
vfU
fL
fU
(m)
0
2
4
6
8
10
12
14
16
18
20
22
24
26
28
30
32
34
Upper Sandy
Rehoboth
Middle Sandstone
Carmel Formation

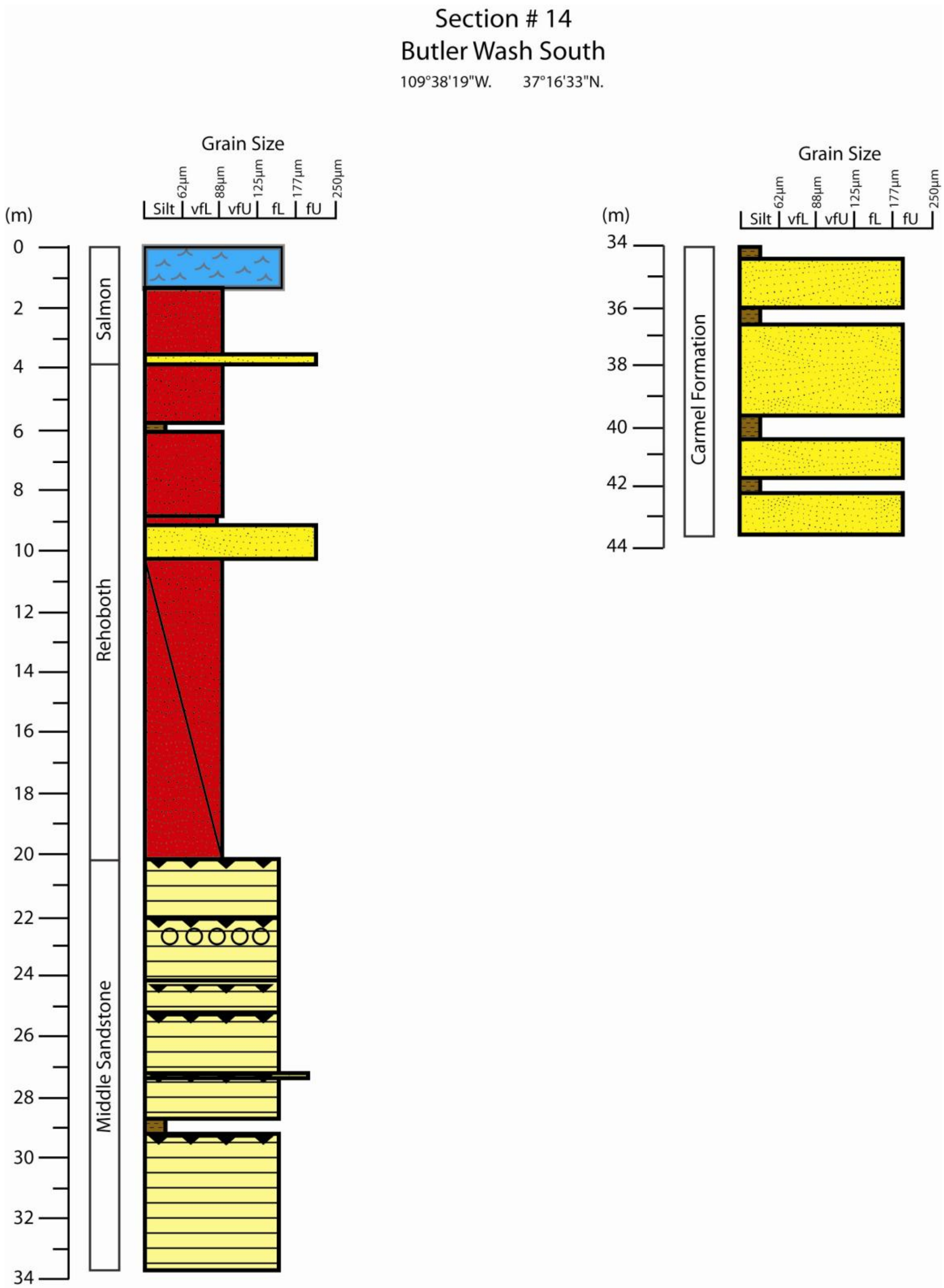
Section # 14
Butler Wash South
109°38'19"W. 37°16'33"N.
Grain Size
62µm
88µm
125µm
177µm
250µm
Silt vfL vfU fL fU
(m)
0
2
4
6
8
10
12
14
16
18
20
22
24
26
28
30
32
34
Salmon
Rehoboth
Middle Sandstone
36
38
40
42
44
Carmel Formation

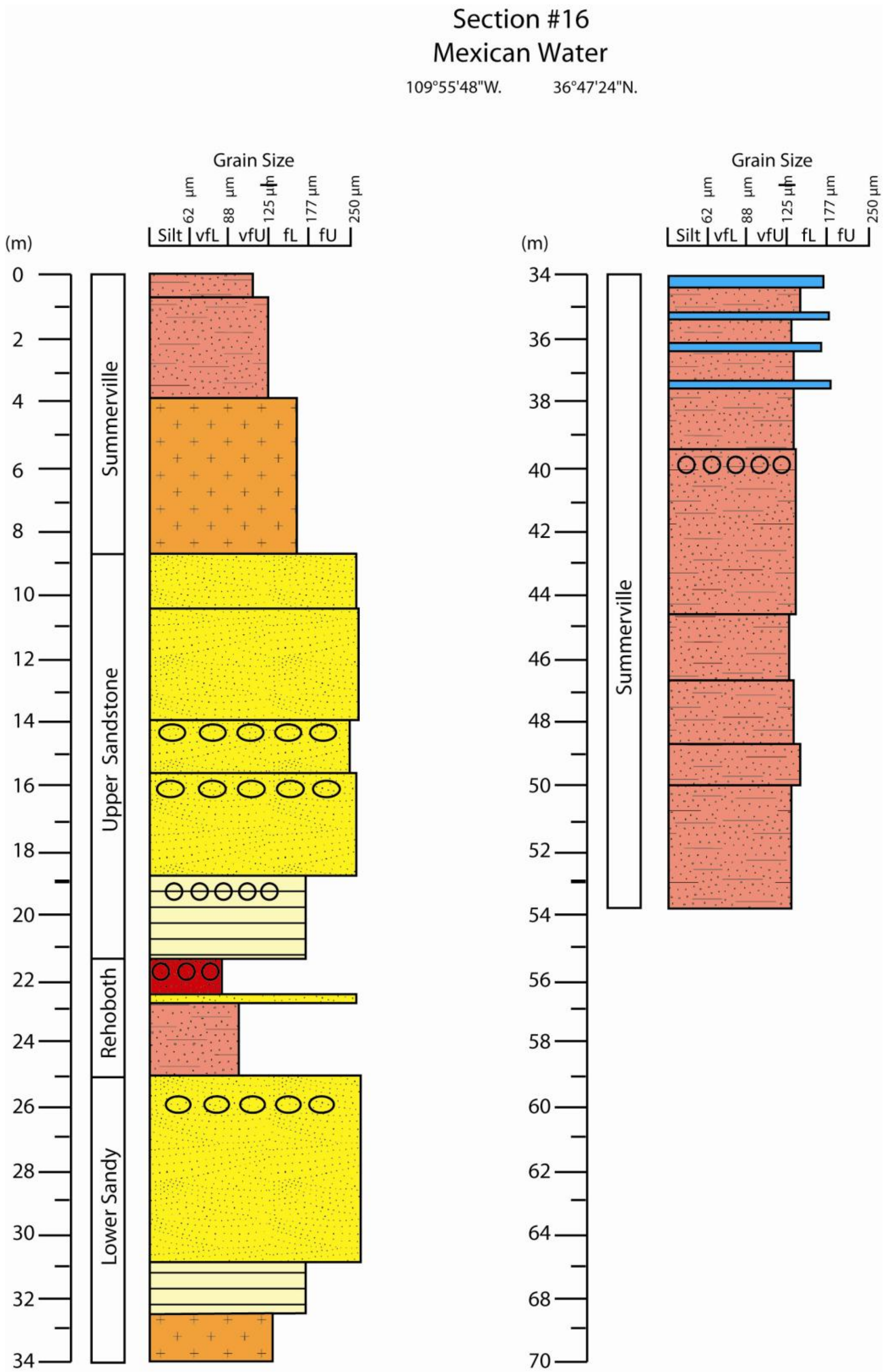

Section #16
Mexican Water
109°55'48"W. 36°47'24"N.
Grain Size
62 µm
88 µm
125 µm
177 µm
250 µm
Silt
vfL
vfU
fL
fU
(m)
Summerville
Upper Sandstone
Rehoboth
Lower Sandy

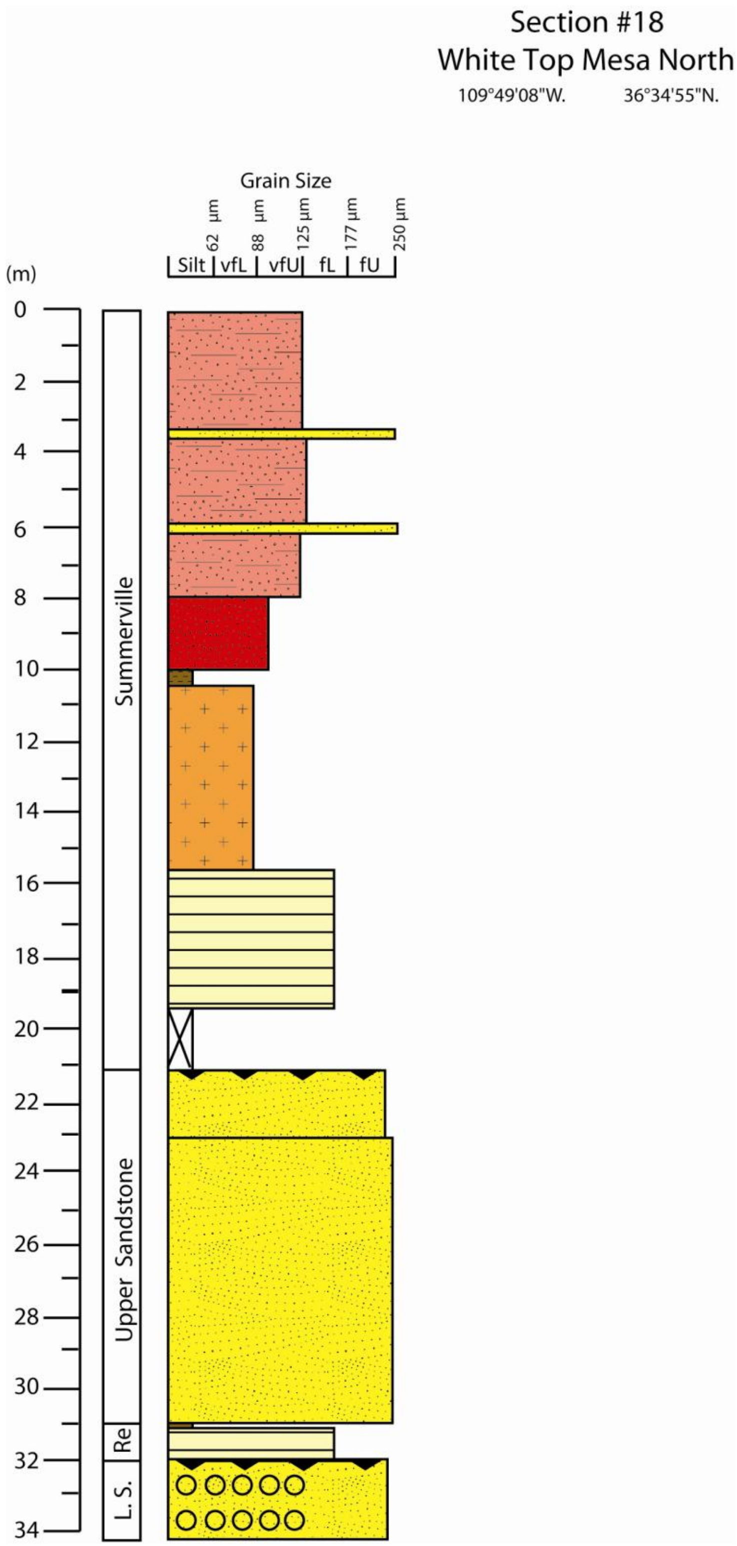

Section #18
White Top Mesa North
109°49'08"W.
36°34'55"N.
Grain Size
62 µm
88 µm
125 µm
177 µm
250 µm
Silt
vfL
vfU
fL
fU
(m)
0
2
4
6
8
10
12
14
16
18
20
22
24
26
28
30
32
34
Summerville
Upper Sandstone
Re
L. S.

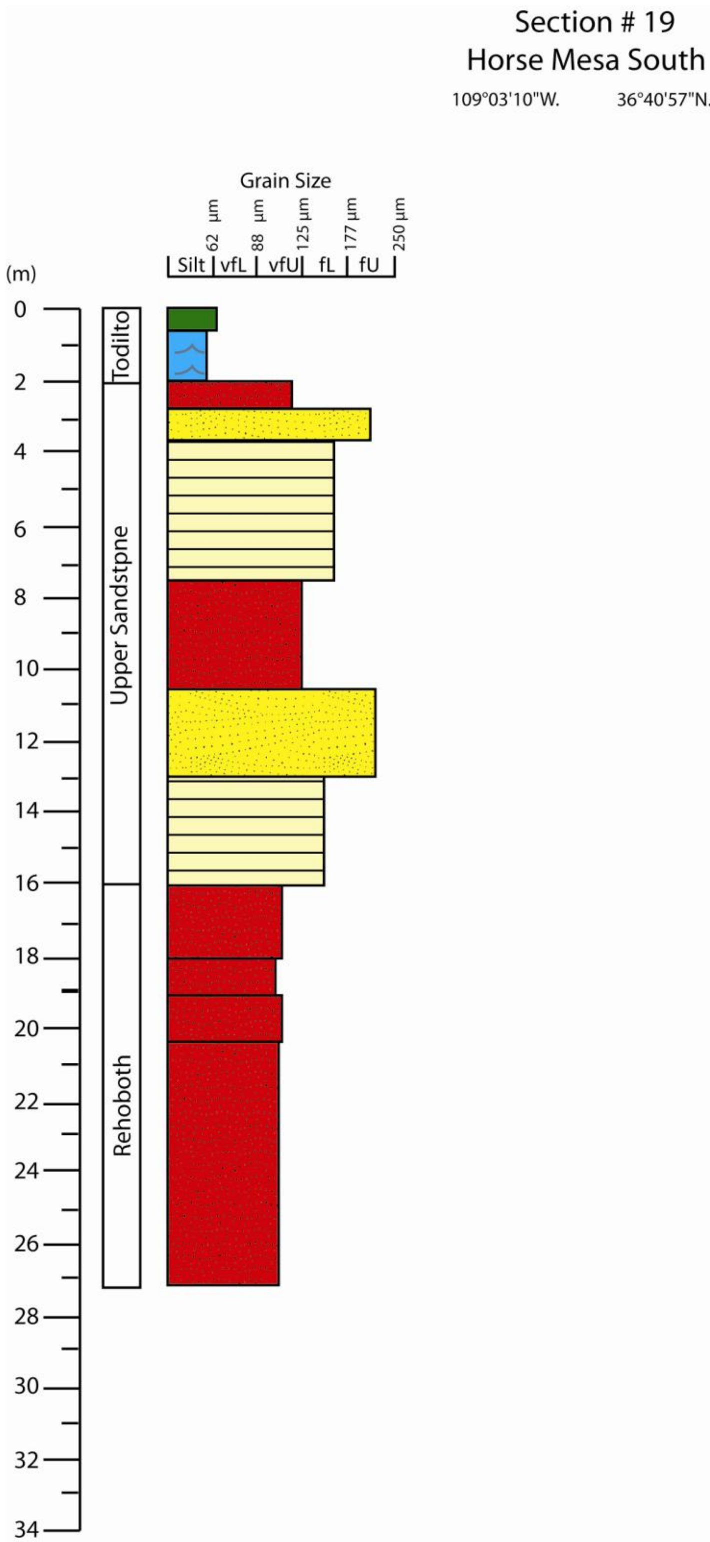
Section # 19
Horse Mesa South
109°03'10"W. 36°40'57"N.
Grain Size
62 µm
88 µm
125 µm
177 µm
250 µm
Silt
vfL
vfU
fL
fU
(m)
0
2
4
6
8
10
12
14
16
18
20
22
24
26
28
30
32
34
Todilto
Upper Sandstpne
Rehoboth

REFERENCES

Anderson, O.J. and **Lucas, S.G.** (1992) The Middle Jurassic Summerville Formation, northern New Mexico. *New Mex.* Geol., **14**, 79-92.

Baars, D.L and others. (1988) Basins of the Rocky Mountain Region. In: *Sedimentary Cover- North American Craton; US. The Geology of North America.* (Ed. L.L. Sloss), Geological Society of America. V. D-2., pp. 109-220.

Barbeau, D.L., (2003) A flexural model for the Paradox Basin: Implications for the tectonics of the Ancestral Rocky Mountains. *Basin Research*., **15**, 97-115.

Benan, C.A.A., and **Kocurek, G.A.** (2000) Catastrophic flooding of an aeolian dune field: Jurassic. Entrada and Todilto Formations, Ghost Ranch, New Mexico, USA *Sedimentology.,* **47***,* 1069-1080.

Blakey, R.C., (1988) Basin tectonics and erg response. In: *Late Paleozoic and Mesozoic Eolian Deposits of the Western Interior of the United States* (Ed. G.A. Kocurek), *Sed. Geol*., **56**, 127-151.

Blakey, R.C., Peterson, F., and **Kocurek, G.A**. (1988) Synthesis of late Paleozoic and Mesozoic eolian deposits of the Western Interior of the United States. *Late Paleozoic and Mesozoic Eolian Deposits of the Western Interior of the United States* (Ed. G.A. Kocurek), *Sed. Geol*., **56**, 3-125.

Carr-Crabaugh, M., and **Kocurek, G.A.** (1998) Continental sequence stratigraphy of a wet eolian system: A key to relative sea-level change. In: *Relative Role of Eustacy, Climate, and Tectonism in Continental Rocks*., SEPM Spec. Publ. **59**, 16 pp.

Cooley, M.E., Harshbarger, J.W., Akers. J.P., and **Hardt, W.F.** (1969) Regional Hydrology of the Navajo and Hopi Indian Reservations, Arizona, New Mexico, and Utah. US Geol. Sur. Prof. Pap., 521-A.

Fryberger, A.G., Hesp, P., and, **Hastings, K**. (1992) Aeolian granule ripple deposits, Namibia. *Sedimentology*., **39**, 319-331.

Geredes, G. Structures left by modern microbial mats in their host sediments. *In: Atlas of microbial mat features preserved within the clastic rock record* (Eds. Schieber, J., Bose, P.K., Eriksson, P.G., Banerjee, S., Sarkar, S., Altermann, W.M., and Catuneau, O.), Elsevier, 5-38.

Glennie, K.W. (1970) *Desert sedimentary environments, developments in sedimentology*, 14, 222 pp. Elsevier, Amsterdam. 5.1, 5.4.5.

Harshbarger, J.W., Repenning, C.A., and **Irwin, J.H.** (1957) Stratigraphy of the uppermost Triassic and Jurassic rocks of Navajo country. *US Geol. Surv. Professional Paper.,* **291**, 74 pp.

Huffmann, C.A. and **Condon, S.M.** (1993) Stratigraphy, structure, and paleogeography of the Pennsylvanian and Permian Rocks, San Juan Basin and adjacent areas, Utah, Colorado, Arizona, and New Mexico. *USGS Bull*., **63**, 953-992.

Imlay, R.W., (1980) Jurassic paleobiogeography of conterminous Unites States and its continental setting. *USGS Prof. Pap*., **1062**, 134 pp.

Johnson, S.Y. (1987) Stratigraphic and sedimentologic studies of Late Paleozoic strata in the Eagle basin and northern Aspen subbasin, northwest Colorado. *US Geol. Surv. Open-File Report* **87-286**, 82 pp.

Johnson, S.Y. (1989) Significance of loessite in the Maroon Formation (Middle Pennsylvanian to Lower Permian), Eagle Basin, northwest Colorado. *J. Sed. Petrol*., **59**, 782-791.

Kelley, V.C. (1950) Regional structure of the San Juan Basin. In: *Guidebook of the San Juan Basin New Mexico and Colorado, New Mexico Geol. Soc. First Field Conference*. pp. 101-108.

Kelley, V.C. (1955) Regional tectonics of the Colorado Plateau and relationships to the origin and distribution of Uranium. *Univ. of New Mexico Publ. in Geol*., **5**: 120 pp.

Kirkland, D.W., Denison, R.E. and **Evans, R.** (1995) Middle Jurassic Todilto Formation of northern New Mexico and southwestern Colorado: Marine or nonmarine. *New Mex. Bur. Min. Meneral Resour. Mem.,* **147,** 37 pp.

Kluth, C.F. and **Coney, P.J.** (1981) Plate Tectonics of the Ancestral Rocky Mountains. *Geology*., **9**, 10-15.

Kocurek, G.A., and **Dott, R.H.** (1983) Jurassic paleogeography and paleoclimate of the central and southern Rocky Mountain region. In: *Mesozoic Paleogeography of the West-Central United States* (Eds M.W. Reynolds and E.D. Dolly), Rocky Mountain Section SEPM, Rockey Mountain Paleogeograph Symposium 2, pp. 101-118.

Kocurek, G.A., and **Nielson, J**. (1986) Conditions favourable for the formation of warm-climate aeolian sand sheets. *Sedimentology*., **33**, 795-816.

Lucas, S.G. and **Anderson, O.J.** (1997) The Jurassic San Rafael Group, Four Corners Region: *New Mex. Geol. Soc. Guidebook*, **48**. 115-132.

Lucas, S.G., Heckert, A.B. and **Anderson, O.J.** (1998) Stratigraphy of the Jurassic Entrada Sandstone in New Mexico (abs). New Mex. Geol. p. 54.

Mallory, W.W. (1972) Regional Synthesis of Pennsylvanian System. In: *Geologic Atlas of the Rocky Mountain Region.* (Ed. W.W. Mallory), Rocky Mountain Assoc. Geol. pp. 111-127.

Mallory, W.W. (1958) Pennsylvanian coarse arkosic redbeds and associated mountains in Colorado. In: *Symposium on Pennsylvanian rocks of Colorado and adjacent areas*. Rocky Mountain Assoc of Geol., pp. 17020.

Mckee et al. (1956) Paleotectonic maps of the Jurassic system. USGS Misc. Geol. Invest. Map I-175.

Ohlen, H.R. and **Mcintyre, L.B.** (1965) Stratigraphic and tectonic features of Paradox Basin, Four Corners Area. *AAPG Bull*., **49**. no. 11., 2020-2040.

O'Sullivan, R.B. (1978) Stratigraphic sections of Middle Jurassic San Rafael Group from Lohali Point, Arizona to Bluff, Utah. US Geol. Surv. Oil and Gas Investigations Chart OC-77.

O'Sullivan, R.B. (1980) Stratigraphic sections of Middle Jurassic San Rafael Group from Wilson Arch to Bluff in southeastern Utah. US Geol. Surv. Oil and Gas Investigations Chart OC-102.

O'Sullivan, R.B., and **Pierce, F.W**. (1983) Stratigraphic diagram of Middle Jurassic San Rafael Group and Associated Formations from the San Rafael Swell to Bluff in Southeastern Utah. US Geol. Surv. Oil and Gas Investigation Chart OC-119.

Parish, J.T. and **Peterson, F.** (1988) Wind directions predicted from global circulation models and wind directions determined from eolian sandstones of the western United States-A comparison. In: *Late Paleozoic and Mesozoic Eolian Deposits of the Western Interior of the United* States, (Ed. G.A. Kocurek) *Sed. Geol.*, **56**, 261-282.

Peterson, F. (1986) Jurassic paleotectonics in the west-central part of the Colorado Plateau, Utah and Arizona. In: *Paleotectonics and Sedimentation* (Ed. J.A. Peterson), Am. Assn. Pet. Geol. Spec. Mem., **41**, pp. 563-596.

Peterson, F. (1988) Pennsylvanian to Jurassic eolian transportation systems in the western United States. In: *Late Paleozoic and Mesozoic Eolian Deposits of the Western Interior of the United States* (Ed. G.A. Kocurek), *Sed. Geol*., **56**, 207-260.

Pipiringos, G.N., and **O'Sullivan, R.B.** (1978) Principal unconformities in Triassic and Jurassic rocks, western interior United States: a preliminary survey. USGS Professional Paper 1035A, pp. A1-A29.

Pye, K. and **Tsoar, H.** (1987) Dust transport and the question of desert loess formation. *Sedimentology*., **34**, 139-153

Pye, K. (1995) The nature, origin, and accumulation of loess. *Quat. Sci. Rev*., **14**. 653-667.

Ridgely, J.L. (1977) Stratigraphy and depositional environments of the Jurassic-Cretaceous sedimentary rocks in the southwest part of the Chama basin, New Mexico. *New Mex. Geol. Surv. Guidebook,* 28th Field Conference-San Juan Basin III, p. 153-158.

Robertson, J.F. and **O'Sullivan, R.B**. (2000) The Middle Jurassic Entrada Sandstone Near Gallup, New Mexico. *The Mountain Geologist*., **38**. no. 2, pp. 53-69.

Robertson, J.F. and **O'Sullivan, R.B**. (2001) The Middle Jurassic Entrada Sandstone Near Gallup, New Mexico: Reply. *The Mountain Geologist*., **38**. no. 4, pp. 228-231.

Soreghan, G.S., Soreghan, M.J., and **Hamilton, M.A.** (2008) Origin and significance of loess in late Paleozoic western Pangaea: A record of tropical cold? *Paleogeog. Paleoclimatol. Paleoecol.,* **268**, 234-259.

Steiner, M.B., (1978) Magnetic Polarity During the Middle Jurassic as Recorded in the Summerville and Curtis Formations., *Earth Planetary Science Letters*, **38**, 331-345.

Stevenson, G.M. and **Baars, D.L.** (1986) The Paradox: A pull-apart basin of Pennsylvanian age. In: *Paleotectonics and sedimentation in the Rocky Mountain region* (J.A. Peterson, ed.), AAPG Memoir, **41**, 513-539.

Wengerd, S.A., and **Matheny, M.L.** (1958) Pennsylvanian system of Four Corners region. *AAPG Bull.*, **42**, 2048-2106.

Woodward, L.A. (1984) Tectonic map of the Rocky Mountain Region of the United States. In: *Mesozoic geology and paleontology of the Four Corners Region* (O.J. Anderson, B.S. Kues, and S.G. Lucas eds.) *New Mex. Geol. Surv Guidebook,* 48th field conference.

Woodard, L.A., Anderson, O.J., and **Lucas, S.G.** (1997) Tectonics of the Four Corners Region of the Colorado Plateau. In: Mesozoic geology and paleontology of the Four Corners Region (O.J. Anderson, B.S. Kues, and S.G. Lucas eds.) *New Mex. Geol. Surv Guidebook,* 48th field conference. 57-64.

Wright, H.E. and **Becker, R.M.** (1951) Correlation of Jurassic Formations along Defiance Monocline, Arizona-New Mexico. *AAPG Bull.,* **35**. no. 3. 607-623.

Ye, H., Royden, L., Burchfiel, C., and **Schuepbach, M.** (1996) Late Paleozoic deformation of interior North America, The Greater Ancestral Rocky Mountains. *AAPG Bull*., **80**, no. 9. 1397-1432.

VITA

Glenn Kenneth Makechnie was born in Boston, Massachusetts, and grew up in New Hampshire. After completing his high school work at Proctor Academy, Andover, New Hampshire in 2000, he entered Brigham Young University in Provo, Utah. Glenn served a two-year mission for the Church of Jesus Christ of Latter-Day Saints in Santa Cruz, Bolivia from 2002-2004. He also played goalie for the Brigham Young University Men's Lacrosse Team during the 2001, 2002, 2005, and 2006 seasons. After completing his BS in Geology at Brigham Young University in August, 2008, Glenn entered the Graduate School at the University of Texas at Austin.

Permanent Address: 14402 Richard Walker Blvd

Austin, TX 78728

This thesis was typed by the author.